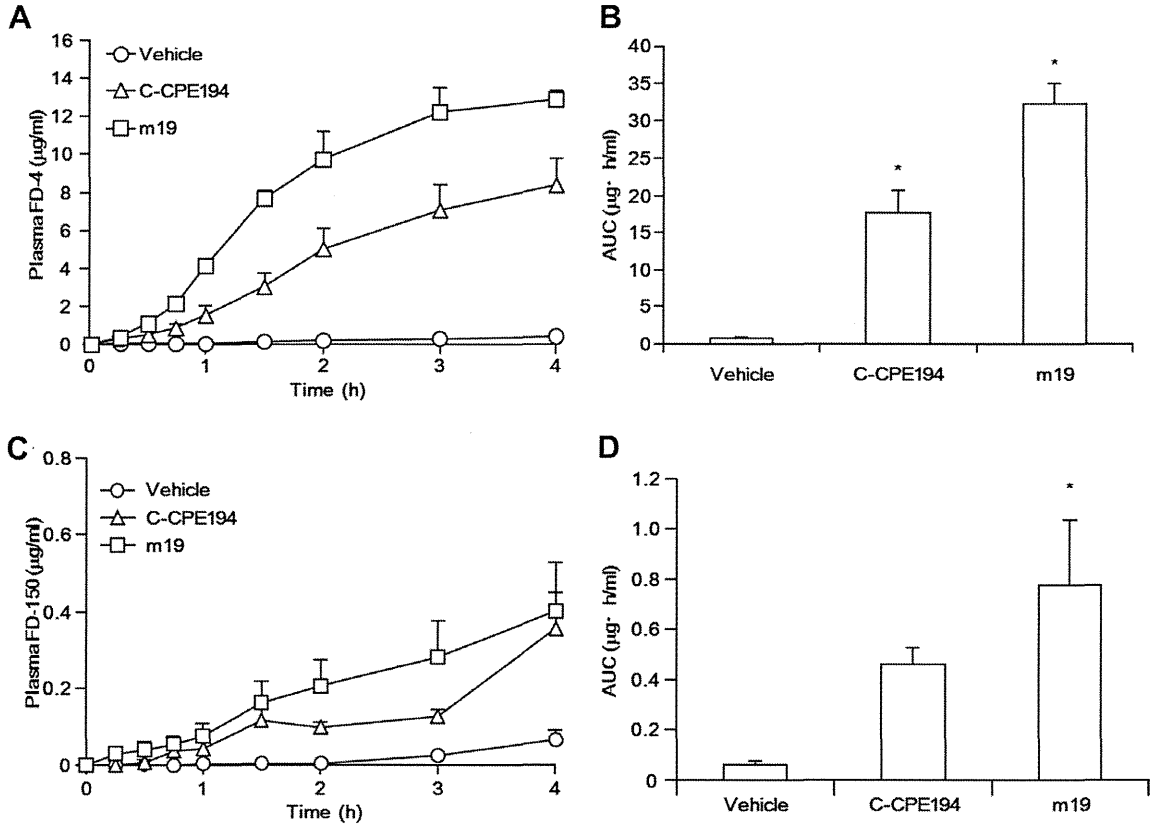

Fig. 2. Jejunal absorption-enhancing effect of C-CPE and m19. Rat jejunum was treated with a mixture of 2 mg of FD-4 (A and B) or FD-150 (C and D) and 0.2 mg of C-CPE or m19. Time-course changes of plasma FD levels were monitored (A and C), and the area under the concentration curve between 0 and 4 h (AUC) was calculated as described in the Section 2 (B and D). Data are means ± SE ($n = 4$). *Significantly different from the vehicle-treated group ($p < 0.05$).

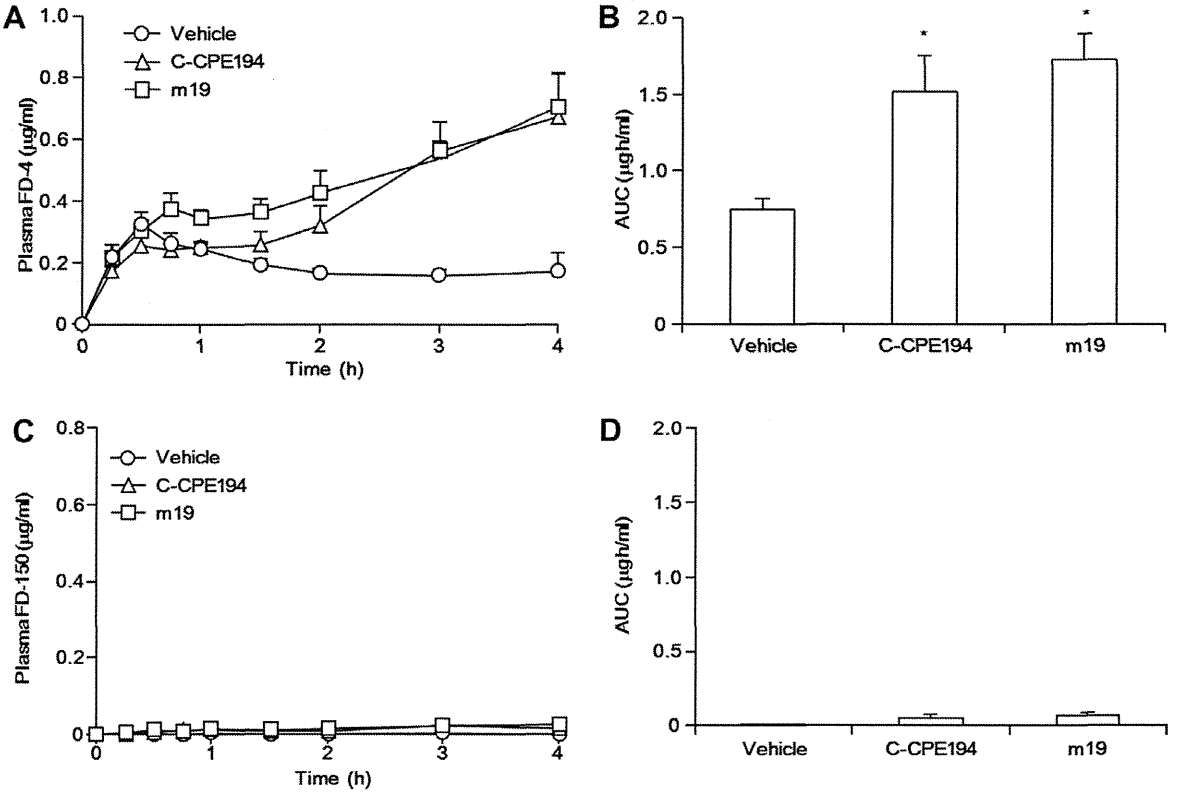

Fig. 3. Nasal absorption-enhancing effect of C-CPE and m19. A mixture of 2 mg of FD-4 (A and B) or FD-150 (C and D) and 0.05 mg of C-CPE or m19 was nasally administrated to rats. Time-course changes of plasma FD levels were monitored (A and C) and AUCs were calculated (B and D). Data are means ± SE ($n = 4$). *Significantly different from the vehicle-treated group ($p < 0.05$).

in both LLC-PK1 and MDCK-II cells. Thus, the properties of the TJ barriers, including the CL expression profiles, may differ between nasal and jejunal mucosa.

CPE binds to CL-3, -4, -6, -7, -8, and -14 [26]. Recently, Kimura et al. showed that CPE also interacts with CL-1 and -2 [27]. Although C-CPE is the receptor-binding domain of CPE, we have not assessed the interaction of C-CPE and m19 with CLs other than CL-1, -2, -4, and -5. A comprehensive understanding of the CL-specificity of C-CPE and m19 is important. However, it is difficult to prepare recombinant CL proteins, and CL-4 is the only CL recombinant protein that has been prepared to date [28]. Yet, we cannot overlook other potential differences in affinity for CLs between C-CPE and m19.

In summary, our findings indicate that mucosal absorption-enhancing activity may be modified by modulating the CL-specificity of CL binders.

Acknowledgments

We thank all members of the laboratory for useful comments and discussion. We also thank Drs. Y. Horiguchi (Osaka University) and S. Tsukita (Kyoto University) for providing us with the C-CPE cDNA and CL-expressing cells, respectively. This work was supported by a Grant-in-Aid for Scientific Research from the Ministry of Education, Culture, Sports, Science and Technology, Japan (21689006, 24390042) and by a Health and Labor Sciences Research Grant from the Ministry of Health, Labor and Welfare of Japan. H.S. is supported by Research Fellowships from the Japan Society for the Promotion of Science for Young Scientists.

References

[1] S. Majumdar, S. Duvvuri, A.K. Mitra, Membrane transporter/receptor-targeted prodrug design: strategies for human and veterinary drug development, Adv. Drug Deliv. Rev. 56 (2004) 1437–1452.
[2] N. Mizuno, T. Niwa, Y. Yotsumoto, Y. Sugiyama, Impact of drug transporter studies on drug discovery and development, Pharmacol. Rev. 55 (2003) 425–461.
[3] M.A. Deli, Potential use of tight junction modulators to reversibly open membranous barriers and improve drug delivery, Biochim. Biophys. Acta 1788 (2009) 892–910.
[4] A. Yamamoto, T. Uchiyama, R. Nishikawa, T. Fujita, S. Muranishi, Effectiveness and toxicity screening of various absorption enhancers in the rat small intestine: effects of absorption enhancers on the intestinal absorption of phenol red and the release of protein and phospholipids from the intestinal membrane, J. Pharm. Pharmacol. 48 (1996) 1285–1289.
[5] L.A. Staehelin, Further observations on the fine structure of freeze-cleaved tight junctions, J. Cell Sci. 13 (1973) 763–786.
[6] M. Furuse, K. Fujita, T. Hiiragi, K. Fujimoto, S. Tsukita, Claudin-1 and -2: novel integral membrane proteins localizing at tight junctions with no sequence similarity to occludin, J. Cell Biol. 141 (1998) 1539–1550.
[7] M. Furuse, S. Tsukita, Claudins in occluding junctions of humans and flies, Trends Cell Biol. 16 (2006) 181–188.
[8] K. Mineta, Y. Yamamoto, Y. Yamazaki, H. Tanaka, Y. Tada, K. Saito, A. Tamura, M. Igarashi, T. Endo, K. Takeuchi, S. Tsukita, Predicted expansion of the claudin multigene family, FEBS Lett. 585 (2011) 606–612.
[9] M. Furuse, M. Hata, K. Furuse, Y. Yoshida, A. Haratake, Y. Sugitani, T. Noda, A. Kubo, S. Tsukita, Claudin-based tight junctions are crucial for the mammalian epidermal barrier: a lesson from claudin-1-deficient mice, J. Cell Biol. 156 (2002) 1099–1111.
[10] T. Nitta, M. Hata, S. Gotoh, Y. Seo, H. Sasaki, N. Hashimoto, M. Furuse, S. Tsukita, Size-selective loosening of the blood–brain barrier in claudin-5-deficient mice, J. Cell Biol. 161 (2003) 653–660.
[11] M. Furuse, K. Furuse, H. Sasaki, S. Tsukita, Conversion of zonulae occludentes from tight to leaky strand type by introducing claudin-2 into Madin–Darby canine kidney I cells, J. Cell Biol. 153 (2001) 263–272.
[12] B.A. McClane, G. Chakrabarti, New insights into the cytotoxic mechanisms of *Clostridium perfringens* enterotoxin, Anaerobe 10 (2004) 107–114.
[13] P.C. Hanna, E.U. Wieckowski, T.A. Mietzner, B.A. McClane, Mapping of functional regions of *Clostridium perfringens* type A enterotoxin, Infect. Immun. 60 (1992) 2110–2114.
[14] J. Katahira, N. Inoue, Y. Horiguchi, M. Matsuda, N. Sugimoto, Molecular cloning and functional characterization of the receptor for *Clostridium perfringens* enterotoxin, J. Cell Biol. 136 (1997) 1239–1247.
[15] N. Sonoda, M. Furuse, H. Sasaki, S. Yonemura, J. Katahira, Y. Horiguchi, S. Tsukita, *Clostridium perfringens* enterotoxin fragment removes specific claudins from tight junction strands: evidence for direct involvement of claudins in tight junction barrier, J. Cell Biol. 147 (1999) 195–204.
[16] M. Kondoh, A. Masuyama, A. Takahashi, N. Asano, H. Mizuguchi, N. Koizumi, M. Fujii, T. Hayakawa, Y. Horiguchi, Y. Watanbe, A novel strategy for the enhancement of drug absorption using a claudin modulator, Mol. Pharmacol. 67 (2005) 749–756.
[17] H. Uchida, M. Kondoh, T. Hanada, A. Takahashi, T. Hamakubo, K. Yagi, A claudin-4 modulator enhances the mucosal absorption of a biologically active peptide, Biochem. Pharmacol. 79 (2010) 1437–1444.
[18] A. Takahashi, E. Komiya, H. Kakutani, T. Yoshida, M. Fujii, Y. Horiguchi, H. Mizuguchi, Y. Tsutsumi, S. Tsunoda, N. Koizumi, K. Isoda, K. Yagi, Y. Watanabe, M. Kondoh, Domain mapping of a claudin-4 modulator, the C-terminal region of C-terminal fragment of *Clostridium perfringens* enterotoxin, by site-directed mutagenesis, Biochem. Pharmacol. 75 (2008) 1639–1648.
[19] A. Takahashi, M. Kondoh, A. Masuyama, M. Fujii, H. Mizuguchi, Y. Horiguchi, Y. Watanabe, Role of C-terminal regions of the C-terminal fragment of *Clostridium perfringens* enterotoxin in its interaction with claudin-4, J. Control. Release 108 (2005) 56–62.
[20] H. Kakutani, A. Takahashi, M. Kondoh, Y. Saito, T. Yamaura, T. Sakihama, T. Hamakubo, K. Yagi, A novel screening system for claudin binder using baculoviral display, PLoS ONE 6 (2011) e16611.
[21] A. Takahashi, Y. Saito, M. Kondoh, K. Matsushita, S.M. Krug, H. Suzuki, H. Tsujino, X. Li, H. Aoyama, K. Matsuhisa, T. Uno, M. Fromm, T. Hamakubo, K. Yagi, Creation and biochemical analysis of a broad-specific claudin binder, Biomaterials 33 (2012) 3464–3474.
[22] M. Furuse, H. Sasaki, S. Tsukita, Manner of interaction of heterogeneous claudin species within and between tight junction strands, J. Cell Biol. 147 (1999) 891–903.
[23] K. Morita, M. Furuse, K. Fujimoto, S. Tsukita, Claudin multigene family encoding four-transmembrane domain protein components of tight junction strands, Proc. Natl. Acad. Sci. USA 96 (1999) 511–516.
[24] H. Chiba, M. Osanai, M. Murata, T. Kojima, N. Sawada, Transmembrane proteins of tight junctions, Biochim. Biophys. Acta 1778 (2008) 588–600.
[25] C.M. Van Itallie, A.S. Fanning, J.M. Anderson, Reversal of charge selectivity in cation or anion-selective epithelial lines by expression of different claudins, Am. J. Physiol. Renal Physiol. 285 (2003) F1078–1084.
[26] K. Fujita, J. Katahira, Y. Horiguchi, N. Sonoda, M. Furuse, S. Tsukita, *Clostridium perfringens* enterotoxin binds to the second extracellular loop of claudin-3, a tight junction integral membrane protein, FEBS Lett. 476 (2000) 258–261.
[27] J. Kimura, H. Abe, S. Kamitani, H. Toshima, A. Fukui, M. Miyake, Y. Kamata, Y. Sugita-Konishi, S. Yamamoto, Y. Horiguchi, *Clostridium perfringens* enterotoxin interacts with claudins via electrostatic attraction, J. Biol. Chem. 285 (2010) 401–408.
[28] L.L. Mitic, V.M. Unger, J.M. Anderson, Expression, solubilization, and biochemical characterization of the tight junction transmembrane protein claudin-4, Protein Sci. 12 (2003) 218–227.

Ann. N.Y. Acad. Sci. ISSN 0077-8923

ANNALS OF THE NEW YORK ACADEMY OF SCIENCES
Issue: *Barriers and Channels Formed by Tight Junction Proteins*

Proof of concept for claudin-targeted drug development

Hidehiko Suzuki, Masuo Kondoh, Azusa Takahashi, and Kiyohito Yagi

Laboratory of Bio-Functional Molecular Chemistry, Graduate School of Pharmaceutical Sciences, Osaka University, Suita, Japan

Address for correspondence: Masuo Kondoh, Ph.D., Laboratory of Bio-Functional Molecular Chemistry, Graduate School of Pharmaceutical Sciences, Osaka University, Suita, Osaka 565-0871, Japan. masuo@phs.osaka-u.ac.jp

Claudins (CLs) are a family of tetra-integral membrane proteins that are a key structural and functional component of tight junctions. CLs are overexpressed in some malignant tumors. Claudin-4 is highly expressed in the epithelial cells covering mucosal immune tissues. CLs may therefore be a potential target for improving drug absorption, treating cancer, and developing mucosal vaccine. Research using *Clostridium perfringens* enterotoxin has resulted in proofs of concept for CL-targeted drug development. A platform for the creation of CL binders, such as immunization of CL and preparation of CL proteins, is now beginning to be established.

Keywords: *Clostridium perfringens* enterotoxin; claudin; mucosal absorption; cancer-targeting; vaccination

Introduction

Epithelium plays a pivotal role in separating the inside and the outside of the body. Drugs must pass across the epithelium to be absorbed; most malignant tumors derive from epithelium, and most pathogens invade the body via the epithelium. Epithelium is therefore a potent target for improving drug absorption, treating cancer, and curing infectious diseases.

Tight junctions (TJs) are intercellular sealing complexes between epithelial cells. TJs prevent the free movement of solutes through the intercellular spaces.[1] Modulation of TJ seals is a popular strategy for improving drug absorption. TJs compartmentalize the apical and basal membrane domains of epithelial cells, leading to the formation of cellular polarity. Loss of cell–cell interaction and cellular polarity, which often occurs in cancer cells during carcinogenesis, leads to exposure of TJ components on the cellular surface.[2] Therefore, TJ components could be potential targets for TJ-targeted drug development.

TJs are composed of biochemical complexes including occludin, claudins (CLs), and junctional adhesion molecules.[3] Treatment with a CL-binding molecule enhanced jejunal absorption of dextran (MW: 4 kDa) 400-fold more than did a currently used clinical absorption enhancer.[4] Expression of CLs is deregulated in malignant tumors.[5,6] CL-expressing epithelium covers mucosal immune tissues.[7] Therefore, CL, a member of a family of tetra-transmembrane proteins, is a promising candidate for TJ-targeted drug development. However, the low immunogenicity and hydrophobicity of CLs make it difficult to determine their structures and prepare CL-binding reagents, including antibodies, thereby delaying CL-targeted drug development.

Claudin-3 (CL-3) and CL-4 are receptors for *Clostridium perfringens* enterotoxin (CPE),[8,9] which causes the symptoms associated with *C. perfringens* type A food poisoning in humans.[10] Half of the C-terminal fragment of CPE (C-CPE) is a receptor-binding domain, and C-CPE is the most frequently used CL-binding molecule.[10] Proof of concept for CL-targeted drug development has been established by using C-CPE as a model CL binder.

Proof of concept for CL-targeted mucosal absorption

Modulation of the epithelial barrier for mucosal absorption of drugs was first explored for TJ-targeted drug development approximately a half

doi: 10.1111/j.1749-6632.2012.06503.x

century ago.[11] Due to the identification of a mucosal absorption-enhancing magnesium and calcium chelator EDTA, modulation of TJs has been a popular strategy for improving drug absorption.[12] However, loosening TJs increases the risk of inducing the nonspecific influx of solutes other than the intended drug. Most researchers therefore think that clinical application is difficult or impossible.

Epithelial cells maintain the intratissue environment not only by preventing the nonspecific influx of solutes through the paracellular space, but also by permitting selective paracellular transport of solutes.[13] Control of the epithelial transport system may reduce the nonspecific influx of solutes during paracellular drug delivery.

There are at least 27 members of the CL family, whose TJ-sealing properties differ depending on the tissues. CL-1 deficiency results in disruption of the epidermal barrier, leading to leakage of small molecules (<600 Da).[14] CL-5–deficient mice exhibited a disrupted blood–brain barrier, which resulted in the influx of solutes (~800 Da).[15] Modulation of CL was proposed as a novel transepithelial drug delivery system by Tsukita and Furuse in the first paper identifying CLs.[16]

C-CPE, a CL-3– and CL-4–binding molecule, is a modulator of TJs.[10] Treatment of jejunum with C-CPE dose dependently enhanced jejunal absorption of dextran (MW: 4 kDa). The absorption-enhancing effect was 400-fold greater than that of sodium caprate, a mucosal absorption enhancer used clinically.[4] Deletion of the CL-binding domains of C-CPE attenuated the absorption-enhancing effect. Sodium caprate also enhanced absorption in the colon, whereas C-CPE did not. C-CPE did not result in any histological injury.[4] Therefore, CL may be a potent target for the development of tissue-specific paracellular transport.

Thirty percent of newly developed drugs are biologics, such as peptides, proteins, and nucleic acids. Because of their low permeability in epithelium, most biologics must be injected into patients. C-CPE has also been shown to enhance nasal, pulmonary, and jejunal absorption of the biologic human parathyroid hormone derivative hPTH(1–34).[17] Taken together, these findings indicate that CLs may be a promising target for improving mucosal absorption of drugs.

Development of a broadly specific CL-binding molecule

CLs form homo- and hetero-type strands on the lateral membrane of the adjacent epithelial cells. Adjacent strands associate with each other resulting in the formation of TJs.[18] The combination of CLs determines the tissue- and solute-specificity of TJs.[14,18] Using CL-binding agents with optimal CL specificity for particular applications likely will reduce the influx of solutes other than the intended drug.

Although CL proteins are needed to screen CL-binding agents, it is difficult to prepare recombinant CL proteins. To our knowledge, CL-4 is the only CL whose recombinant protein is able to be prepared. Display of protein on a viral surface is one method of membrane protein preparation.[19,20] Budded baculovirus (BV) display large amounts of membrane proteins on the surface in their active form.[21,22] CL-4 is displayed on the BV membrane (Fig. 1).[23] When a mixture of CL-4–bound phages and negative

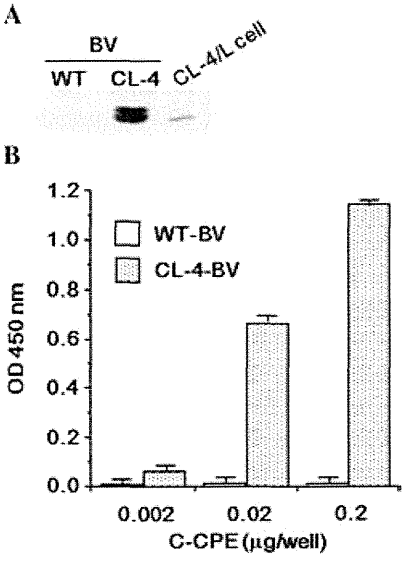

Figure 1. Preparation of CL-4–displaying BV. (A) Western blot analysis. Wild-type BV (WT-BV) and CL-4–BV (0.1 μg/lane) were subjected to SDS-PAGE followed by immunoblot analysis with anti–CL-4 antibody. The lysate of CL-4–expressing L (CL-4/L) cells was used as the positive control. (B) Interaction of a CL-4 binder with CL-4–BV. Immunotubes were coated with WT-BV or CL-4–BV, and C-CPE was added to the BV-coated immunotubes at the indicated concentration. C-CPE bound to the BV-coated tubes was detected by using ELISA with an anti-his-tag antibody. Data are means ± SD ($n = 3$).

control phages is added to the tube coated with CL-4–displaying BV, CL-bound phages were enriched (data not shown). Therefore, CL-displaying BV may be a screening reagent for obtaining candidate CL-binding molecules.

Functional domain mapping of C-CPE revealed that the 16 amino acids of the C-terminal are critical for the binding of C-CPE to CL-4 and that alanine-substituted C-CPE mutants showed either increased or decreased affinity to CL-4.[24,25] We prepared a C-CPE mutant library in which the affinity-increasing residues were randomly replaced by 20 amino acids. CL-1–binding mutants were selected by using CL-1–displaying BV. Interestingly, one of the CL-1–binding mutants also bound to CL-2, CL-4, and CL-5 (data not shown). The broadly specific CL binder was a more potent TJ modulator and jejunal absorption enhancer than was C-CPE (data not shown).

CL-targeted cancer therapy

Abnormal expression of CLs often occurs in human malignancies, such as breast, prostate, ovarian, gastric, and pancreatic cancers.[6,26] Moreover, deregulation of CL expression is associated with metastasis.[27,28] Intratumoral administration of a CL-targeting toxin, CPE, suppresses tumor growth in mice inoculated with CL-4–expressing human pancreatic cancer cell line Panc-1.[26,29] Intracranial administration of CPE inhibited tumor growth in murine brain metastasis model using the human breast cancer cell line MDA-MB-468 or the murine breast cancer cell line NT2.5 without any apparent local or systemic toxicity.[5] Therefore, CL may be a potential target for cancer therapy.

We prepared C-CPE–fused protein synthesis inhibitory factor (PSIF) derived from *Pseudomonas aeruginosa* exotoxin A and found that C-CPE–PSIF is a CL-4–targeting molecule.[30] Intratumoral administration of C-CPE–PSIF suppressed tumor growth in murine breast cancer cell line 4T1.[31] Injection of C-CPE–PSIF also inhibited tumor growth and spontaneous lung metastasis of murine breast cancer without any apparent side effects.[32] CL-3 and/or CL-4 is expressed in various tissues, such as lung, intestine, liver, and kidney. Most CLs in normal cells are contained within the TJ complexes, whereas localization of CLs is deregulated in some cancers.[6,26] The human colon carcinoma cell line Caco-2 forms a polarized cell monolayer with well-developed TJs when cells reach confluence. This cell line is often used as a model of polarized normal epithelial cell sheets.[33] The polarized cells are more resistant to C-CPE–PSIF treatment than are nonpolarized cells (Fig. 2). C-CPE–PSIF was more cytotoxic to membrane-seeded polarized cells that were treated from the apical side than the basal side.[31] Therefore, CL-targeting molecules may recognize deregulation of cellular polarity, which could lead to fewer side effects.

Proof of concept for CL-targeted mucosal vaccination

Approximately 20 million people die every year from infectious diseases. Most pathogens invade the body through the mucosal epithelium. A standard strategy for overcoming infectious diseases is the prevention of entry of pathogens through the epithelium and the elimination of infected cells. Vaccination strategies are classified as either parenteral or

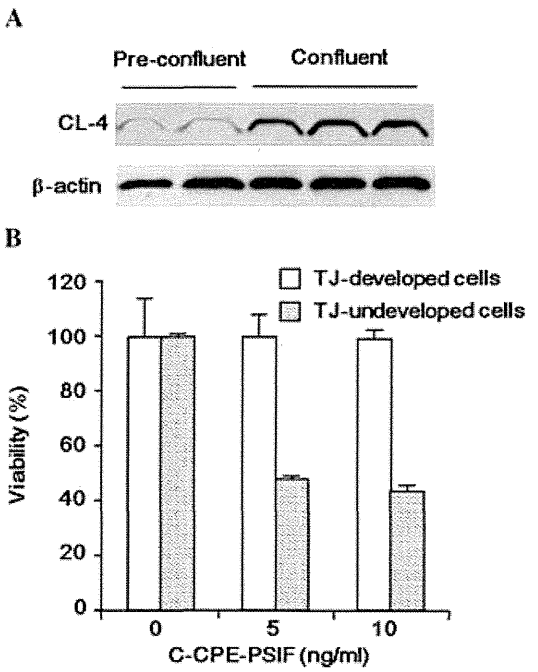

Figure 2. Cytotoxic specificity of C-CPE–PSIF. To develop tight TJs, Caco-2 monolayer cells were grown at confluency for three days. To maintain loose TJs, Caco-2 cells were seeded at subconfluency. The cell lysates were subjected to SDS-PAGE followed by Western blotting with CL-4 antibody (A). The cells were treated with the indicated concentrations of C-CPE–PSIF for 48 h, and then cell viability was measured by WST-8 assay (B). Data are means ± SD ($n = 3$).

mucosal. Parenteral vaccinations activate systemic immune responses, leading to elimination of infected cells. Mucosal vaccinations activate both the systemic and mucosal immune responses, leading to both prevention of the entry of pathogens through the mucosal epithelium and elimination of infected cells.[34–36] Mucosal administration is generally considered the least painful route of administration. Mucosal vaccination is an ideal vaccination strategy; however, mucosal administration of antigen proteins alone often does not activate immune responses.

There are mucosa-associated lymphoid tissues (MALTs) in the intestine, nose, and lungs, as follows: gut-associated lymphoid tissues (GALTs), nasopharynx-associated lymphoid tissues (NALTs), and bronchus-associated lymphoid tissues (BALTs), respectively.[37,38] Antigen-presenting cells, B cells, and T cells, underlie MALTs. Therefore, efficient delivery of antigens into MALTs is one strategy for mucosal vaccination. CL-4 is highly expressed in epithelial cells covering GALTs and NALTs.[7,39] Nasal administration of C-CPE–fused ovalbumin (OVA) induced production of OVA-specific serum IgG and nasal, vaginal, and fecal IgA (Fig. 3, data not shown). A mixture of C-CPE and OVA did not potentiate these immune responses (data not shown). Deletion of the CL-binding domain of OVA–C-CPE attenuated activation of the immune responses. Nasal immunization with OVA–C-CPE showed antitumor activity in mice inoculated with OVA-expressing thymoma cells.[39] Therefore, CL-4–targeting may be a potential strategy for developing mucosal vaccination. C-CPE is a fragment of enterotoxin that is stable in the gastrointestinal tract. C-CPE is a promising lead binder for the development of orally administered vaccines.

Perspective

C-CPE is the most frequently used CL-binding molecule and was 400-fold more potent at enhancing absorption than was an alternative absorption enhancer used clinically. The CL-targeting toxin showed *in vitro* and *in vivo* antitumor activity without any apparent side effects. Nasal immunization with the CL-targeting antigen activated both systemic and mucosal immune responses. Thus, we have demonstrated proof of concept for CL-targeted mucosal absorption, cancer-targeting, and mucosal vaccination by using C-CPE as a CL ligand.

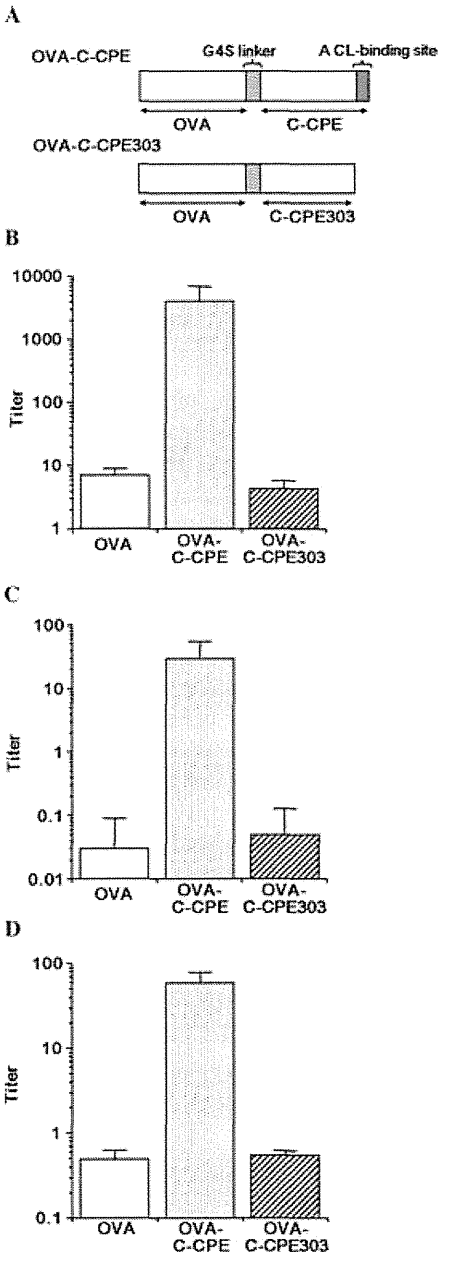

Figure 3. Involvement of CL-4 in immune responses to OVA–C-CPE. (A) Schematic illustration of OVA–C-CPE and its mutant. The C-terminal 16 amino acid-deleted C-CPE mutant (C-CPE303) did not bind to CL-4.[25] To clarify the involvement of CL-4 in the immune response initiated by OVA–C-CPE, OVA was fused with C-CPE303, resulting in OVA–C-CPE303. (B–D) immune responses by OVA–C-CPE or OVA–C-CPE303. Mice were nasally immunized with OVA, OVA–C-CPE, or OVA–C-CPE303 (5 μg OVA) once a week for three weeks. Seven days after the last immunization, the levels of OVA-specific serum IgG (B), nasal IgA (C), and vaginal IgA (D) were measured by ELISA. Data are means ± SD ($n = 4$).

C-CPE is a fragment of enterotoxin. Repeat administration of C-CPE showed production of C-CPE–specific serum IgG and mucosal IgA.[40] Development of biocompatible CL binders, such as chemicals, peptides, and antibodies is needed for future clinical application. CL has very short extracellular loops: the first extracellular loop is approximately 50 amino acids; the second loop is approximately 10 amino acids. CLs are hydrophobic proteins, and preparation of a recombinant protein is currently possible for CL-4 only, and synthetic peptides corresponding to the extracellular loop domains do not fully work as a screening source for CL binders (our unpublished data). Therefore, the development of CL binders, including antibodies, has been very slow. Recently, immunization of autoimmune-prone mice with CL-expressing cells and of rats with CL-coding DNA led to the successful preparation of anti–CL-4 and anti–CL-1 monoclonal antibodies, respectively.[41,42] Importantly, anti–CL-4 antibody showed therapeutic antitumor activity *in vitro* and *in vivo*. Anti–CL-1 antibody inhibited infection of hepatic cells by hepatitis C virus.[41] A dual-targeting monoclonal antibody against CL-3 and CL-4 has also been prepared.[43] CL-displaying BV was developed as a screening reagent for CL binders.[23] A broadly specific CL binder was developed by using a C-CPE library and CL-displaying BV. Thus, the development of CL binders has begun. Proof of concept for CL-targeted drug development is yet to be fully established, but we believe that in the future, step by step, CL-modulating and CL-targeting technology will lead to the clinical application of CL-targeted pharmaceutical therapies.

Acknowledgments

This work was supported in part by a Grant-in-Aid for Scientific Research from the Ministry of Education, Culture, Sports, Science, and Technology of Japan (21689006) and by Health and Labor Sciences Research Grants from the Ministry of Health, Labor, and Welfare of Japan. H.S. and A.T. were supported by Research Fellowships from the Japan Society for the Promotion of Science for Young Scientists.

Conflicts of interest

We declare no conflict interest significant enough to influence the results or interpretation of the submitted paper.

References

1. Powell, D.W. 1981. Barrier function of epithelia. *Am. J. Physiol.* **241:** G275–G288.
2. Wodarz, A. & I. Nathke. 2007. Cell polarity in development and cancer. *Nat. Cell Biol.* **9:** 1016–1024.
3. Schneeberger, E.E. & R.D. Lynch. 2004. The tight junction: a multifunctional complex. *Am. J. Physiol.* **286:** C1213–C1228.
4. Kondoh, M., A. Masuyama, A. Takahashi, *et al.* 2005. A novel strategy for the enhancement of drug absorption using a claudin modulator. *Mol. Pharmacol.* **67:** 749–756.
5. Kominsky, S.L., B. Tyler, J. Sosnowski, *et al.* 2007. *Clostridium perfringens* enterotoxin as a novel-targeted therapeutic for brain metastasis. *Cancer Res.* **67:** 7977–7982.
6. Morin, P.J. 2005. Claudin proteins in human cancer: promising new targets for diagnosis and therapy. *Cancer Res.* **65:** 9603–9606.
7. Tamagawa, H., I. Takahashi, M. Furuse, *et al.* 2003. Characteristics of claudin expression in follicle-associated epithelium of Peyer's patches: preferential localization of claudin-4 at the apex of the dome region. *Lab. Invest.* **83:** 1045–1053.
8. Morita, K., M. Furuse, K. Fujimoto, *et al.* 1999. Claudin multigene family encoding four-transmembrane domain protein components of tight junction strands. *Proc. Natl. Acad. Sci. USA* **96:** 511–516.
9. Sonoda, N., M. Furuse, H. Sasaki, *et al.* 1999. *Clostridium perfringens* enterotoxin fragment removes specific claudins from tight junction strands: evidence for direct involvement of claudins in tight junction barrier. *J. Cell Biol.* **147:** 195–204.
10. McClane, B.A. 1992. *Clostridium perfringens* enterotoxin: structure, action and detection. *J. Food Saf.* **12:** 237–252.
11. Windsor, E. & G.E. Cronheim. 1961. Gastro-intestinal absorption of heparin and synthetic heparinoids. *Nature.* **190:** 263–264.
12. Aungst, B.J. 2000. Intestinal permeation enhancers. *J. Pharm. Sci.* **89:** 429–442.
13. Van Itallie, C.M. & J.M. Anderson. 2006. Claudins and epithelial paracellular transport. *Annu. Rev. Physiol.* **68:** 403–429.
14. Furuse, M., M. Hata, K. Furuse, *et al.* 2002. Claudin-based tight junctions are crucial for the mammalian epidermal barrier: a lesson from claudin-1-deficient mice. *J. Cell Biol.* **156:** 1099–1111.
15. Nitta, T., M. Hata, S. Gotoh, *et al.* 2003. Size-selective loosening of the blood-brain barrier in claudin-5-deficient mice. *J. Cell Biol.* **161:** 653–660.
16. Furuse, M., H. Sasaki, K. Fujimoto, *et al.* 1998. A single gene product, claudin-1 or -2, reconstitutes tight junction strands and recruits occludin in fibroblasts. *J. Cell Biol.* **143:** 391–401.
17. Uchida, H., M. Kondoh, T. Hanada, *et al.* 2010. A claudin-4 modulator enhances the mucosal absorption of a biologically active peptide. *Biochem. Pharmacol.* **79:** 1437–1444.
18. Furuse, M. & S. Tsukita. 2006. Claudins in occluding junctions of humans and flies. *Trends Cell Biol.* **16:** 181–188.

19. Loisel, T.P., H. Ansanay, S. St-Onge, *et al.* 1997. Recovery of homogeneous and functional beta 2-adrenergic receptors from extracellular baculovirus particles. *Nat. Biotechnol.* **15:** 1300–1304.
20. Strehlow, D., S. Jodo & S.T. Ju. 2000. Retroviral membrane display of apoptotic effector molecules. *Proc. Natl. Acad. Sci. USA* **97:** 4209–4214.
21. Hayashi, I., Y. Urano, R. Fukuda, *et al.* 2004. Selective reconstitution and recovery of functional gamma-secretase complex on budded baculovirus particles. *J. Biol. Chem.* **279:** 38040–38046.
22. Masuda, K., H. Itoh, T. Sakihama, *et al.* 2003. A combinatorial G protein-coupled receptor reconstitution system on budded baculovirus. Evidence for Galpha and Galphao coupling to a human leukotriene B4 receptor. *J. Biol. Chem.* **278:** 24552–24562.
23. Kakutani, H., A. Takahashi, M. Kondoh, *et al.* 2011. A novel screening system for claudin binder using baculoviral display. *PLoS One.* **6:** e16611.
24. Takahashi, A., E. Komiya, H. Kakutani, *et al.* 2008. Domain mapping of a claudin-4 modulator, the C-terminal region of C-terminal fragment of *Clostridium perfringens* enterotoxin, by site-directed mutagenesis. *Biochem. Pharmacol.* **75:** 1639–1648.
25. Takahashi, A., M. Kondoh, A. Masuyama, *et al.* 2005. Role of C-terminal regions of the C-terminal fragment of *Clostridium perfringens* enterotoxin in its interaction with claudin-4. *J. Control. Release.* **108:** 56–62.
26. Kominsky, S.L. 2006. Claudins: emerging targets for cancer therapy. *Expert Rev. Mol. Med.* **8:** 1–11.
27. Agarwal, R., T. D'Souza & P.J. Morin. 2005. Claudin-3 and claudin-4 expression in ovarian epithelial cells enhances invasion and is associated with increased matrix metalloproteinase-2 activity. *Cancer Res.* **65:** 7378–7385.
28. Dhawan, P., A.B. Singh, N.G. Deane, *et al.* 2005. Claudin-1 regulates cellular transformation and metastatic behavior in colon cancer. *J. Clin. Invest.* **115:** 1765–1776.
29. Michl, P., M. Buchholz, M. Rolke, *et al.* 2001. Claudin-4: a new target for pancreatic cancer treatment using *Clostridium perfringens* enterotoxin. *Gastroenterology* **121:** 678–684.
30. Ebihara, C., M. Kondoh, N. Hasuike, *et al.* 2006. Preparation of a claudin-targeting molecule using a C-terminal fragment of *Clostridium perfringens* enterotoxin. *J. Pharmacol. Exp. Ther.* **316:** 255–260.
31. Saeki, R., M. Kondoh, H. Kakutani, *et al.* 2009. A novel tumor-targeted therapy using a claudin-4-targeting molecule. *Mol. Pharmacol.* **76:** 918–926.
32. Saeki, R., M. Kondoh, H. Kakutani, *et al.* 2010. A claudin-targeting molecule as an inhibitor of tumor metastasis. *J. Pharmacol. Exp. Ther.* **334:** 576–582.
33. Meunier, V., M. Bourrie, Y. Berger, *et al.* 1995. The human intestinal epithelial cell line Caco-2; pharmacological and pharmacokinetic applications. *Cell Biol. Toxicol.* **11:** 187–194.
34. Boyaka, P.N., M. Marinaro, J.L. Vancott, *et al.* 1999. Strategies for mucosal vaccine development. *Am. J. Trop. Med. Hyg.* **60:** 35–45.
35. Cardenas-Freytag, L., E. Cheng & A. Mirza. 1999. New approaches to mucosal immunization. *Adv. Exp. Med. Biol.* **473:** 319–337.
36. Michels, K.B. & H. zur Hausen. 2009. HPV vaccine for all. *Lancet*. **374:** 268–270.
37. Kiyono, H. & S. Fukuyama. 2004. NALT- versus Peyer's-patch-mediated mucosal immunity. *Nat. Rev. Immunol.* **4:** 699–710.
38. Kunisawa, J., S. Fukuyama & H. Kiyono. 2005. Mucosa-associated lymphoid tissues in the aerodigestive tract: their shared and divergent traits and their importance to the orchestration of the mucosal immune system. *Curr. Mol. Med.* **5:** 557–572.
39. Kakutani, H., M. Kondoh, M. Fukasaka, *et al.* 2010. Mucosal vaccination using claudin-4-targeting. *Biomaterials.* **31:** 5463–5471.
40. Suzuki, H., M. Kondoh, X. Li, *et al.* 2011. A toxicological evaluation of a claudin modulator, the C-terminal fragment of *Clostridium perfringens* enterotoxin, in mice. *Pharmazie.* **66:** 543–546.
41. Fofana, I., S.E. Krieger, F. Grunert, *et al.* 2010. Monoclonal anti-claudin 1 antibodies prevent hepatitis C virus infection of primary human hepatocytes. *Gastroenterology.* **139:** 953–964.
42. Suzuki, M., M. Kato-Nakano, S. Kawamoto, *et al.* 2009. Therapeutic antitumor efficacy of monoclonal antibody against Claudin-4 for pancreatic and ovarian cancers. *Cancer Sci.* **100:** 1623–1630.
43. Kato-Nakano, M., M. Suzuki, S. Kawamoto, *et al.* 2010. Characterization and evaluation of the antitumour activity of a dual-targeting monoclonal antibody against claudin-3 and claudin-4. *Anticancer Res.* **30:** 4555–4562.

Biomaterials 33 (2012) 3464–3474

Contents lists available at SciVerse ScienceDirect

Biomaterials

journal homepage: www.elsevier.com/locate/biomaterials

Creation and biochemical analysis of a broad-specific claudin binder

Azusa Takahashi [a,1], Yumiko Saito [a,1], Masuo Kondoh [a,*,1], Kyohei Matsushita [a], Susanne M. Krug [b], Hidehiko Suzuki [a], Hirofumi Tsujino [c], Xiangru Li [a], Hiroshi Aoyama [c], Koji Matsuhisa [a], Tadayuki Uno [c], Michael Fromm [b], Takao Hamakubo [d], Kiyohito Yagi [a]

[a] Laboratory of Bio-Functional Molecular Chemistry, Graduate School of Pharmaceutical Sciences, Osaka University, Suita, Osaka 565-0871, Japan
[b] Institute of Clinical Physiology, Charite, Campus Benjamin Franklin, Freie University and Humboldt University, Berlin, Germany
[c] Laboratory of Analytical Chemistry, Graduate School of Pharmaceutical Sciences, Osaka University, Suita, Osaka 565-0871, Japan
[d] Department of Molecular Biology and Medicine, Research Center for Advanced Science and Technology, The University of Tokyo, Meguro, Tokyo 153-8904, Japan

ARTICLE INFO

Article history:
Received 26 December 2011
Accepted 9 January 2012
Available online 7 February 2012

Keywords:
Claudin
Drug delivery system
Baculovirus
Phage display
Tight junction

ABSTRACT

Claudins (CL) are a family of tetra-transmembrane proteins that are the structural and functional components of tight junctions (TJ). CLs are promising targets for drug development because of their role in mucosal drug absorption and cancer. However, CL-targeted drug development has been delayed because CLs have low antigenicity and preparing CL proteins is difficult. We developed a CL binder by using the C-terminal fragment of *Clostridium perfringens* enterotoxin (C-CPE) and a baculoviral display system. After screening CL binders from a C-CPE mutant-displaying library by using CL-displaying budded baculovirus (BV) we isolated a C-CPE mutant called m19, which bound to CL1, CL2, CL4 and CL5. A 3-dimensional analysis showed that m19 has a structural backbone similar to C-CPE. The charge density of the CL-binding domains of m19 and C-CPE differed, suggesting that electrostatic interactions may occur between m19 and CLs. Treatment of epithelial cells with m19 decreased the paracellular but not transcellular integrity, and m19 enhanced jejunal absorption. Thus, we successfully created a CL binder with broad specificity. These findings will contribute to future preparation of CL binders for CL-targeted drug development.

1. Introduction

Epithelia covers the body surface and prevents entry of xenobiotics and pathogens into the body. The most critical role of epithelium is to form a barrier separating the body from the environment. Tight junctions (TJs) are located in the apical part of the lateral membranes and seal the intercellular space to prevent free movement of solutes via the paracellular spaces by forming points of fusion between the membranes [1].

Modulation of TJ-seals has been investigated as a strategy to improve drug absorption [2]. Most malignant tumors are derived from epithelium. The early stages of cancer are frequently associated with the loss of intercellular adhesion and cellular polarity [3]. Mucosal vaccination is a promising therapy for infectious diseases [4]. Many studies have investigated the efficient delivery of antigens to mucosal immune tissues in epithelium [5,6]. Therefore, epithelia are promising therapeutic targets for drug absorption, infectious diseases, and cancer.

A series of biochemical analyses of TJs revealed that intercellular TJ-seals contains transmembrane proteins, such as occludin, tricellulin, the family of claudin (CL) and junction adhesion molecule [7]. CLs are estimated to be the primary structural and functional components of the TJ-seal. Mammalian CLs are a family of 27 known tetra-transmembrane proteins [8,9]. CLs form homo- and hetero-type strands on the cell membrane, and adjacent CL strands interact with those on the lateral membrane, leading to the formation of TJ-seals [10]. The properties of the TJ-barrier are determined by a combination of CL proteins. CL1- and CL5-deficient mice show disruption of the epidermal barrier and the blood–brain barrier, respectively [11,12]. Some malignant tumors, including

Abbreviations: CL, claudin; TJ, tight junction; C-CPE, C-terminal fragment of *Clostridium perfringens* enterotoxin; BV, budded baculovirus; CPE, *Clostridium perfringens* enterotoxin; TBS, Tris-buffered saline; SDS-PAGE, sodium dodecyl sulfate-polyacrylamide gel electrophoresis; PCR, polymerase chain reaction; PBS, phosphate-buffered saline; ELISA, enzyme-linked immunosorbent assay; FACS, fluorescence activated cell sorting; TEER, transepithelial electrical resistance; FD-4, fluorescein isothiocyanate-labeled dextran with a molecular mass of 4 kDa; AUC, area under the curve.

* Corresponding author. Laboratory of Bio-Functional Molecular Chemistry, Graduate School of Pharmaceutical Sciences, Osaka University, Suita, Osaka 565-0871, Japan. Tel.: +81 6 6879 8196; fax: +81 6 6879 8199.
E-mail address: masuo@phs.osaka-u.ac.jp (M. Kondoh).

[1] These authors equally contributed to this study.

0142-9612/$ – see front matter © 2012 Elsevier Ltd. All rights reserved.
doi:10.1016/j.biomaterials.2012.01.017

pancreatic, breast and lung cancers overexpress CLs [13]. Epithelial cells covering mucosal immune tissues express CL4 [14,15]. CL1 is a co-receptor for hepatitis C virus [16]. These findings strongly indicate that CLs may be a strong candidate for epithelium-targeted drug development. However, CLs have low antigenicity and preparing CL proteins is difficult, so that the development of CLs binders has been slow.

Clostridium perfringens enterotoxin (CPE), a 35-kDa polypeptide, is a food poison that is lethal to humans [17]. CPE has an N-terminal cytotoxic domain and a C-terminal receptor binding domain (C-CPE) [18,19]. The CPE receptors are identical to those on CL3 and CL4 [18,20]. C-CPE contains 184-319 amino acids and was the only known nontoxic CL3/4 binder before 2005 [20]. CPE has high affinity to CL3 and CL4 with a Ka value of approximately $1.0 \times 10^8\ M^{-1}$ [21]. Modulation of TJ-barriers by using the CL binders C-CPE and part of the N-terminally truncated mutants enhances jejunal, nasal and pulmonary absorption of drugs [22,23]. We prepared CL binders fused to protein synthesis inhibitory factor derived from *Pseudomonas aeruginosa* exotoxin, and found that a CL-targeting toxin showed antitumor activity [24–26]. C-CPEs were used to develop an efficient system to deliver antigen to mucosal immune tissue [27]. CPE shows antitumor activity against brain and pancreatic tumors with no apparent side effects [28,29]. These findings indicate that ligands for CLs may be promising molecules for drug development.

We previously determined the functional domain of the C-CPEs, and prepared a phage library displaying C-CPE mutants, in which the functional amino acid residues were randomly altered [30–32]. Developing a screening system for CL binders was necessary because it is difficult to prepare CL proteins. Budded baculovirus (BV) displays membrane proteins on its surface in an active form [33,34], and we already found that CL-displaying BV provides a screen for CL binders [30]. In the present study, we screened CL binders from the C-CPE mutant library by using CL-displaying BV.

2. Materials and methods

2.1. Cell culture

A mouse fibroblast cell line (L cells) and mouse CL1, CL2, CL4 or CL5-expressing L cells (CL1/L cells, CL2/L cells, CL4/L cells, CL5/L cells) were kindly provided by Dr. S. Tsukita (Kyoto University, Kyoto, Japan). Sf9 cells and Caco-2 cells were obtained from Invitrogen (Gaithersburg, MD) and ATCC cell bank (Manassas, VA), respectively. L cells were maintained in modified Eagle's medium supplemented with 10% fetal bovine serum (FBS) in a 5% CO_2 atmosphere at 37 °C. Huh7 cells were cultured in Dulbecco's modified Eagle's medium (DMEM) supplemented with 10% FBS. The cells were maintained in a 5% CO_2 atmosphere at 37 °C. Mock or bicellularly tricellulin-overexpressing MDCK II cells (MDCK V1 or MDCK TRa-8) were maintained in DMEM supplemented with 400 μg/ml G418, 10% FBS, 100 μg/ml streptomycin (Invitrogen) [35].

2.2. Recombinant BV construction and Sf9 cell culture

Mouse CL1, CL4 and CL5 cDNAs were kindly provided by Dr. M. Furuse (Kobe University, Japan). Recombinant BV was prepared by using the Bac-to-Bac expression system, according to the manufacturer's instructions (Invitrogen). Briefly, CL cDNA were inserted into pFastBac1, and the resulting plasmids were transduced into DH10Bac *E. coli* cells. Recombinant bacmid DNA was extracted from the cells. Sf9 cells were transduced with the bacmid encoding CL, and the recombinant BV was recovered by centrifugation of the conditioned medium [25].

2.3. Preparation of the BV fractions

Sf9 cells (2×10^6 cells) were infected with recombinant BV at a multiplicity of infection of 5. The BV fraction was recovered from the culture supernatant of infected Sf9 cells by centrifugation 72 h after infection. The pellets of the BV fraction were resuspended in Tris-buffered saline (TBS) containing 1% protease inhibitor cocktail (Sigma-Aldrich, St. Louis, MO) and stored at 4 °C until used. The expression of CL1 and CL4 in the BV was confirmed by sodium dodecyl sulfate-polyacrylamide gel electrophoresis (SDS-PAGE) and an immunoblot analysis with anti-CL antibodies (Invitrogen).

2.4. Preparation of mutant C-CPE library

A C-CPE mutant-displaying phage library was prepared as described previously [30]. Briefly, C-CPE fragments in which the functional amino acids (S304, S305, S307, N309, S313 and K318) [31] were randomly mutated were prepared by PCR with pET-H_{10}PER as a template and primers with triplet codons coding the functional amino acids randomly changed to triplet codons coding any of the 20 amino acids. The PCR fragments were inserted into a phagemid. The resultant phagemid containing the C-CPE mutant library was transduced into *E. coli* TG1 cells, and the cells were stored at −80 °C.

2.5. Preparation of phage

TG1 cells containing the phagemid coding C-CPE mutant library were cultured in 2YT medium (Invitrogen) containing 2% glucose and ampicillin. M13K07 helper phages (Invitrogen) were added when the cells reached the growth phase, and the medium was changed to 2YT medium containing ampicillin and kanamycin. The cells were cultured an additional 6 h and the phages in the conditioned medium were precipitated with polyethylene glycol. The phages were suspended in NTE buffer (100 mM NaCl, 10 mM Tris, 1 mM EDTA) and stored at 4 °C until use.

2.6. Screening of phages using BV

CL1-BVs (0.5 μg protein) were adsorbed onto an immunotube (Nunc, Roskilde, Denmark). The C-CPE phage library was transferred to the BV-coated tubes, and the tubes were washed 15 times with phosphate-buffered saline (PBS) containing 0.05% Tween 20. The phages bound to the tube were eluted with 100 mM HCl. TG1 cells were infected with the eluted phages; the phages had been prepared as described above. The resulting phages were subjected to repeated selection using the CL1-BV-coated immunotubes. We performed sequencing analysis with a 5′-gtaaat-gaattttctgtatgagg-3′ primer to identify the isolated phage clones.

2.7. Measurement of phage titer

We measured the titer (colony formation unit (CFU)/ml) of the phage solution to quantify the concentration of phages. Briefly, the phage solution was diluted to 10^{-5}–10^{-10} with 2YT containing 2% glucose. The diluted solution was infected with TG1 cells, and the cells were seeded onto Petrifilm™ (Tech-Jam, Osaka, Japan). The colonies were counted after 16 h of incubation, and the titer was calculated.

2.8. Purification of C-CPE mutants

The plasmids containing C-CPE mutants derived from the CL1-bound phage clones were prepared by PCR-amplifying the C-CPE mutant fragments with the phagemid coding C-CPE mutants as template, a common forward primer (5′-ggaattccatatggatatagaaaaagaaatccttgatttagctg-3′, the *Nde*I site is underlined), and a reverse primer for C-CPE mutants (5′-cgcggatcc<u>ttaaaacttttgaaataatat-3′</u>, the *BamH*I site is underlined). The site-directed C-CPE mutant fragments were cloned by PCR with C-CPE or C-CPE mutants as template. The resulting PCR fragment was inserted into pET16b, and the sequence was confirmed. The plasmids were transduced into *E. coli* strain BL21 (DE3), and production of mutant C-CPEs was induced by the addition of isopropyl-D-thiogalactopyranoside. The harvested cells were lysed in buffer A (10 mM Tris-HCl, pH 8.0, 400 mM NaCl, 5 mM $MgCl_2$, 0.1 mM phenylmethanesulfonyl fluoride, 1 mM 2-mercaptoethanol, and 10% glycerol). The lysates were applied to HiTrap™ Chelating HP (GE Healthcare, Buckinghamshire, UK), and mutant C-CPEs were eluted with buffer A containing imidazole. The buffer was exchanged with PBS by using a PD-10 column (GE Healthcare), and the purified protein was stored at −80 °C until used. Purification of the mutant C-CPEs was confirmed by SDS-PAGE, followed by staining with Coomassie Brilliant Blue. Protein was quantified with a BCA protein assay kit with bovine serum albumin as standard (Pierce Chemical, Rockford, IL).

2.9. Enzyme-linked immunosorbent assay (ELISA)

The BV-displaying CLs were diluted with TBS and adsorbed to the wells of 96-well immunoplates (Nunc, Roskilde, Denmark) overnight at 4 °C. The wells were washed with PBS and blocked with TBS containing 4% BlockAce (Dainippon Sumitomo Pharma, Osaka, Japan) for 2 h at room temperature. The phages or C-CPEs were added to the well and incubated for an additional 2 h at room temperature. The wells were washed with PBS and incubated with anti-M13 antibody or anti-His-tag antibody for 2 h at room temperature. The immunoreactive proteins were detected by an HRP-labeled secondary antibody with 3,3′,5,5′-tetramethylbenzine as substrate. The reaction was terminated by the addition of 1 M H_2SO_4, and the optical density of the immunoreactive proteins were measured at 450 nm.

2.10. Fluorescence-activated cell sorting

The CLs/L cells were incubated with C-CPEs for 1 h at 4 °C, followed by incubation with an anti C-CPEs-fused tag antibody. The cells were incubated

with fluorescein-labeled secondary antibody, and the C-CPEs-bound cells were detected and analyzed with a flow cytometer (FACScalibur, Becton Dickinson, New Jersey, USA).

2.11. Crystallization

Initial screening of crystallization conditions was performed by sitting drop vapor diffusion using the JBScreen Crystal Screening Kit (Jena Bioscience GmbH, Jena, Germany) by mixing equal volumes of m19 and well solution. Drops were equilibrated against the well solution at 25 °C. The crystals used in the analysis were obtained by mixing 1 μl of protein solution at 9 mg/ml, 1 μl of reservoir solution containing 0.1 M sodium acetate, pH 4.6 and 1.75 M ammonium sulfate, and allowing the drop to equilibrate against 1 ml of reservoir solution by the hanging drop method.

2.12. Data collection, phasing, and refinement

X-ray diffraction data on the m19 crystals were collected at 100 K in a nitrogen stream, after the crystals were soaked with 3.4 M sodium malonate pH 5.0 as a cryoprotectant. X-ray data were collected from a single crystal at 2.0 Å with a Raynoix MX225HE CCD detector on the beamline BL44XU at SPring-8 (Table 1). The x-ray wavelength was 0.9 Å, the angle oscillation range was 1.0, and the crystal-to detector distance was 230 mm.

The diffraction data were processed using the programs iMOSFLM [36] and SCALA [37] from the CCP4 suite [38]. m19 structure was solved by molecular replacement method using the program BALBES [39] and the atomic coordinates of C-CPE (PDB ID : 2QUO). The model was examined and manually fitted based on the 2Fo − Fc and Fo − Fc electron density maps using the program COOT [40]. Isotropic restrained refinement was performed using the program REFMAC5 [41]. Data collection and refinement statistics are shown in Table 1.

2.13. Transepithelial electrical resistance (TEER)

Caco-2 cells were seeded in BD BioCoat™ Fibrillar Collagen Cell Culture Inserts (BD Biosciences, Franklin Lakes, NJ) at a subconfluent density. The TEER of the Caco-2 monolayer cell sheets on the chamber was monitored using a Millicell-ERS epithelial volt-ohmmeter (Millipore, Billerica, MA). The Caco-2 monolayers were cultured for 5 days, and then treated with C-CPE or C-CPE mutants on the basal side of the insert. Changes in TEER values were monitored. The TEER values were normalized by the area of the Caco-2 monolayer, and the TEER value of a blank Transwell™ chamber (background) was subtracted.

Table 1
Data collection and refinement statistics.

Synchrotron/beamline	SPring-8/BL44XU
Crystal parameters	
Space Group	$P\,3_1\,2\,1$
Cell dimensions (Å)	$a = b = 87.63$, $c = 63.9$
Angles (°)	$\alpha = \beta = 90$, $\gamma = 120$
Data collection	
Wavelength (Å)	0.9
Resolution limit (Å)	37.94–2.00 (2.10–2.00)
R_{merge}	0.082 (0.962)
Total number of observations	213,338 (30,794)
Total number of unique	19,504 (2,827)
Observations	
Mean $I/\sigma I$	14.8 (2.5)
Completeness	99.4 (100.0)
Multiplicity	10.9 (10.9)
Refinement	
Protein atoms in model	989
Solvent atoms in model	66
$R_{working}$	0.233
R_{free}	0.252
Rmsd from ideal geometry	
Bond length (Å)	0.025
Bond angles (°)	2.315
Ramachandran plot (%)	
Most favored	95.9
Outlier	4.1

Values for the outermost resolution shell are given in parentheses.
$R_{merge} = \sum_{hkl} \sum_i |I_i(hkl) - \{ I(hkl) \}| / \sum_{hkl} \sum_i I_i(hkl)$, where $I_i(hkl)$ is the intensity of the ith observation of reflection hkl and $\{ I(hkl) \}$ is the average over all observations of reflection hkl.
$R_{working} = \sum_{hkl} || F_{obs} |-|F_{calc} || / \sum_{hkl} |F_{obs}|$, where F_{obs} and F_{calc} are the observed and calculated structure-factor amplitudes, respectively.
R_{free} is $R_{working}$ calculated using 5% of the date that were omitted from refinement.

MDCK V1 or MDCK TRa-8 cells were seeded on porous polycarbonate microwell inserts (Millicell-HA, Millipore; 0.6-cm^2 area) and were grown to confluence. After 4 days, the cells were treated with C-CPE or C-CPE mutants on the basal side of the insert. TEER were determined before and 2 h after addition of C-CPEs. Values were normalized and background was subtracted.

2.14. Two-path impedance spectroscopy

Two-path impedance spectroscopy was performed as described previously [42]. Briefly, this method is based on a model describing the epithelial resistance, R^{epi}, as a parallel circuit consisting of the transcellular resistance, R^{trans}, and the paracellular resistance, R^{para}. The subepithelial resistance, R^{sub}, is in series to R^{epi} and here is caused by the filter support. The apical and the basolateral membranes of the confluent cell layer are represented by resistors and capacitors in parallel (R^a, C^a, and R^b, C^b, respectively). R^a and R^b add up to R^{trans}. A spectrum of alternating currents was applied (35 μA/cm^2, frequency range 1.3–65 kHz), and changes in tissue voltage were detected by phase-sensitive amplifiers (402 frequency response analyzer, Beran Instruments, Gilching, Germany; 1286 electrochemical interface; Solartron Schlumberger, Farnborough, United Kingdom). Complex impedance values (Z_{real}, $Z_{imaginary}$) were calculated and plotted in a Nyquist diagram. R^{trans} and R^{para} were determined from experiments in which impedance spectra and fluxes of fluorescein as a paracellular marker substance were obtained before and after chelating extracellular Ca^{2+} with EGTA. This caused TJs to partially open and to increase fluorescein flux. In separate experiments it has been demonstrated that changes of fluorescein fluxes are inversely proportional to R^{epi} changes (data not shown)

2.15. Immunohistochemistry and confocal fluorescence microscopy

After cells were grown to confluence on on porous polycarbonate microwell inserts (Millicell-HA, Millipore) and treated with C-CPE or m19 as described above. The inserts were rinsed with PBS, and fixed with methanol they were permeabilized with PBS containing 0.5% (vol/vol) Triton X-100. Primary antibodies were diluted: mouse anti-FLAG-M2 (Sigma-Aldrich) 1:500; rabbit anti-occludin (Invitrogen) 1:200; guinea pig anti-tricellulin 1:1000; Alexa Fluor 488 goat anti-guinea pig (Pineda-Antikörper-Service, Berlin, Germany [35]), 1:2000; secondary antibodies were: Alexa Fluor 488 goat anti-mouse; Alexa Fluor 594 goat anti-rabbit, 1:500 (Molecular Probes, Hamburg, Germany; MoBiTec). Immunofluorescence images were obtained with a confocal laser scanning microscope (LSM 510 Meta, Carl Zeiss, Jena, Germany), using excitation wavelengths of 543 and 488 nm.

2.16. Flux measurements of fluorescein isothiocyanate-dextran (FD-4)

All flux studies were performed in Ussing chambers under short-circuit conditions. For FD-4 fluxes, Ussing chambers were filled with 10 ml Ringer's per side, 50 μl of pre-dialyzed FD-4 (molecular mass ~4 kDa, 20 mM) were added apically, and basolateral samples (300 μl) were replaced with fresh Ringer's 0, 15, 30, 45, and 60 min after addition. Samples were analyzed with a fluorometer (Spectramax Gemini, Molecular devices) at 520 nm (fluorescein). Fluxes were calculated as increase in tracer quantity (corrected for dilution) per time unit and filter area (0.6 cm^2). Permeabilities were calculated as flux/concentration on the donor side.

2.17. In situ loop assay

Jejunal absorption of FD-4 was evaluated using an *in situ* loop assay as described previously [23]. The experiments were performed according to the guidelines of the Ethics Committee of Osaka University. Eight-week-old Wistar male rats were anesthetized with pentobarbital, a midline abdominal incision was

Table 2
Sequences of CL1-binding phage clones.

	304	305	307	309	313	318
C-CPE	Ser	Ser	Ser	Asn	Ser	Lys
m5	Arg	Ala	Pro	Arg	His	Asn
m9	Arg	Arg	Arg	Arg	Arg	Lys
m10	Arg	Ser	Ala	Arg	Lys	Lys
m11	Arg	Val	Arg	Arg	Arg	Lys
m17	Leu	Pro	Arg	Arg	Lys	Gln
m19	Ala	Pro	Arg	His	His	Lys
m21	Ala	Pro	Arg	Asp	Arg	Lys
m24	Arg	Arg	Gln	Gln	Arg	Lys
m36	Arg	Pro	Arg	Arg	His	Lys
m37	Arg	Pro	Arg	Phe	His	Gln
m86	Thr	Pro	Arg	Arg	His	Lys
m89	Ala	Pro	Arg	Ala	Arg	Thr

The top row shows the sequences of the randomly mutated amino acids of C-CPE. The left-most column is the clone numbers of the CL1-bound phages.

made, and the jejunum was washed with PBS. A 5-cm long jejunal loop was prepared by closing both ends with sutures. A mixture of FD-4 (2 mg) and C-CPEs was injected into the jejunal loop. Blood was collected from the jugular vein at the indicated time points. The plasma levels of FD-4 were measured with a fluorescence spectrophotometer (Tristar LBP941; Berthold Technologies, Bad Wildbad, Germany). The AUC of FD-4 from 0 to 6 h ($AUC_{0-6\ h}$) was calculated by the trapezoidal method.

3. Results

3.1. Screening of CL1 binders from the C-CPE mutant library

CL1 is a promising target for modulation of the mucosal and epidermal barrier, and cancer-targeting [11,13,43–45]. Therefore, we attempted to screen CL1 binders by using a C-CPE mutant-displaying phage library and CL1-BV. We prepared CL1-BV (Suppl. Fig. 1A). The C-CPE library was added to CL1-BV-adsorbed tubes, and the CL1-BV-bound phages were recovered (1st screening). We repeated this screening process two more times (2nd and 3rd screening). The ratio of the incubated phage titers to the recovered phage titers, measured to determine the enrichment of CL1-bound phages, increased during screening from 0.172×10^{-6} to 2.69×10^{-6}, indicating the efficiency of our screening system for CL1 binders (Suppl. Fig. 1B). We isolated CL1-binding phage clones after the 3rd screening, and investigated the interaction of each monoclonal phage with CL1-BV (Suppl. Fig. 1C).

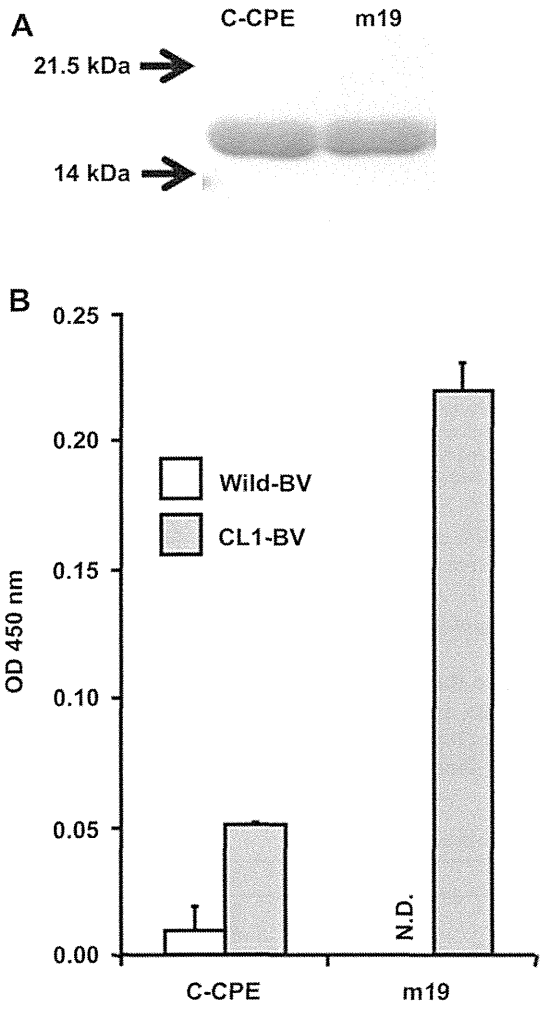

Fig. 1. Interaction of C-CPE mutants with CL1-BV. A) Purification of m19. m19 was expressed in *E. coli* and isolated by nickel-affinity chromatography. The purification of proteins was confirmed by SDS-PAGE. The putative molecular mass of C-CPEs is approximately 15 kDa. B) Interaction of m19 with CL1. m19 (2.0 μg) was added to wild-BV- or CL1-BV-coated immunoplates, followed by detection of C-CPE mutants bound to each type of BV. Data are presented as means ± SD ($n = 3$). N.D., not detected.

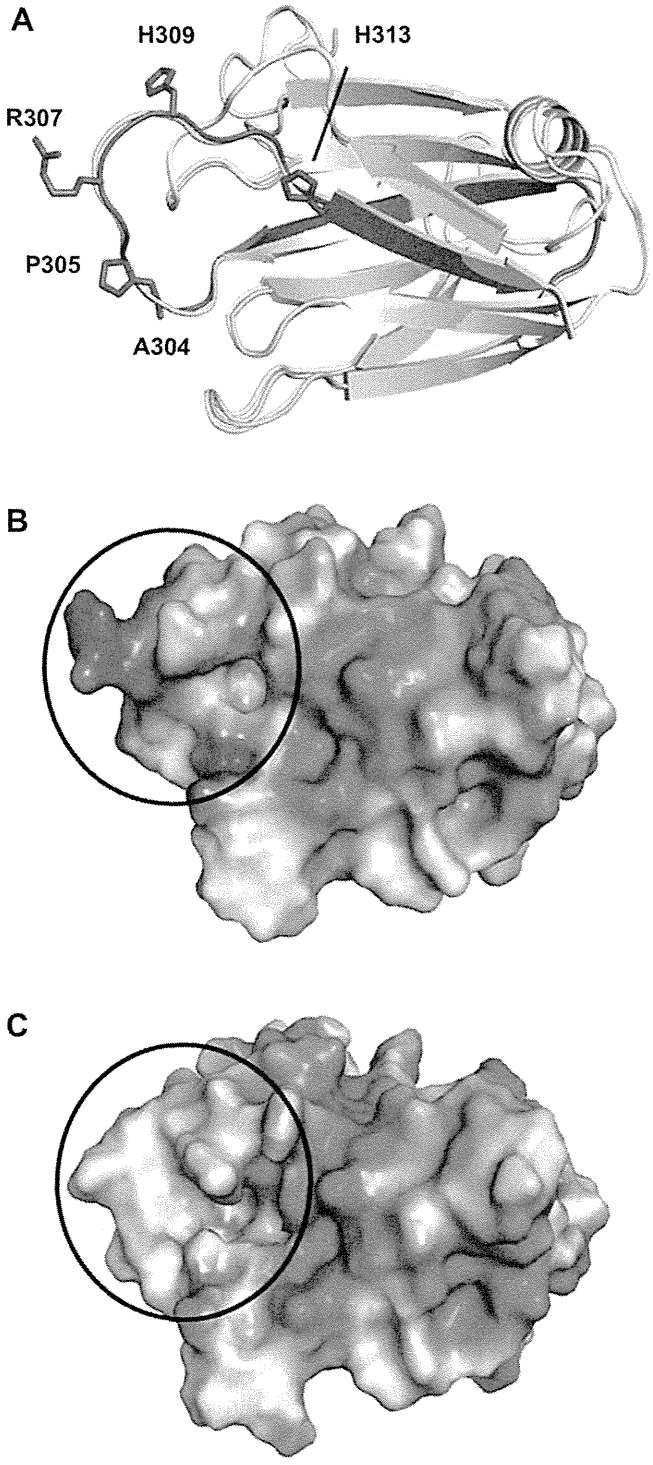

Fig. 2. The structure of m19. A) Superpositioning of m19 structure (yellow) on C-CPE (gray, PDB ID code 2QUO). The Cα rmsd for the superposition is 1.61 Å. The COOH-terminal 30 residues of m19, including β8 and β9 sheets and the intervening surface loop, are shown dark red. The mutated residues of m19 are shown as stick model. B, C) Electrostatic potential surface of m19 (B) and C-CPE (C). The color red, white, and blue indicate negative, neutral and positive charges, respectively. The circle indicates the putative CL-binding region [47].

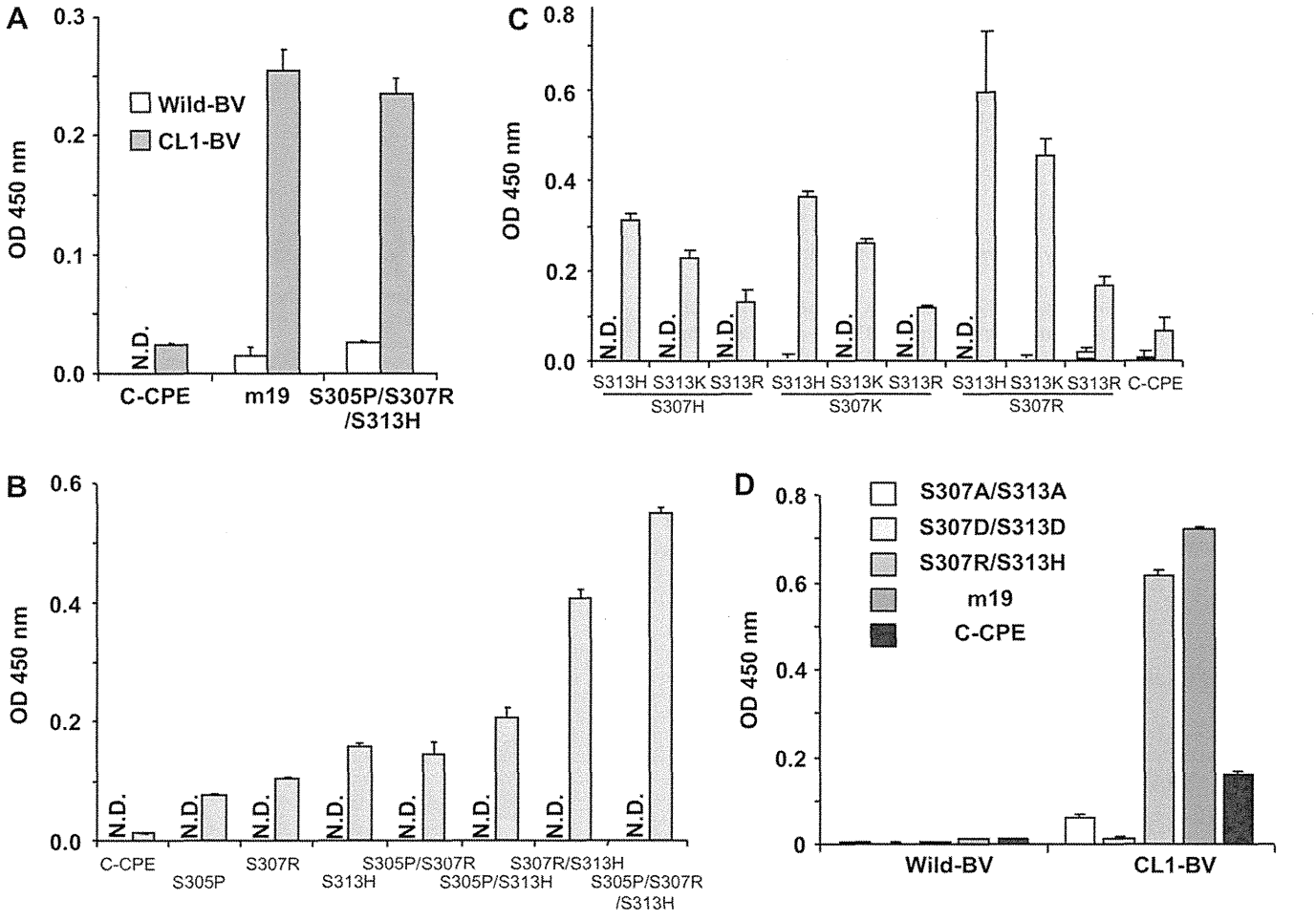

Fig. 3. Identification of the functional amino acids associated with CL1-binding to m19. A) Interaction of C-CPE, m19, or triple mutated C-CPE with CL1. C-CPE, m19 or the triple mutated C-CPE (2.0 μg) was added to wild-BV- or CL1-BV-coated immunoplates, followed by detection of binding to each type of BV. Data are presented as means ± SD ($n = 3$). B) Interaction of C-CPE or single or double-substituted C-CPE mutants with CL1. C-CPE or C-CPE mutants (2.0 μg) were added to wild-BV- or CL1-BV-coated immunoplates, followed by detection of binding to each type of BV. Data are presented as means ± SD ($n = 3$). C) Effects of a positive charge in C-CPE at positions 307 and 313 on interaction between C-CPE mutants and CL1-BV. C-CPE or C-CPE mutants (2.0 μg) was added to wild-BV- or CL1-BV-coated immunoplates, followed by detection of binding to each type of BV. Data are presented as means ± SD ($n = 3$). N.D., not detected. D) Effects of a negative charge in C-CPE at positions 307 and 313 on interaction between C-CPE mutants and CL1-BV. C-CPE or C-CPE mutants (2.0 μg) were added to wild-BV- or CL1-BV-coated immunoplates, followed by detection of binding to each type of BV. Data are presented as means ± SD ($n = 3$).

We analyzed the sequences of the CL1-BV-bound phages and identified CL1-binder candidates with amino acid sequences that differed from the wild-type sequence (Table 2). We prepared the recombinant proteins and investigated their interaction with CL1 by ELISA with CL-BVs (Fig. 1). m19, m36 and m86 were CL1 binders (data not shown on m36 and m86).

3.2. Structure of m19

We determined the three-dimensional structure of m19 to clarify why m19 bound to CL1. The structure of m19 was solved to a resolution of 2.00 Å by using molecular replacement method using the atomic coordinates of C-CPE (PDB ID : 2QUO). The final model has good stereochemistry and an R_{free} of 25.2%. A full summary of the data and refinement statistics is included in Table 1.

m19 has a structural backbone that is similar to C-CPE (Fig. 2A). Each protein contains 9 β-sheets and one α-helix. The loop domain between the β 8- and β 9-sheets is the putative CL binding domain [46]. Their loop domains have the same backbone (Fig. 2A). In contrast, the electrostatic map of the binding pocket region differed between C-CPE and m19 (Fig. 2B). The substitution of Ser with Ala, Ser with Pro, Ser with Arg, Asn with His and Ser with His at positions 304, 305, 307, 309 and 313, respectively, resulted in a more positive charge in the putative CL binding domain.

3.3. Functional domain mapping of m19

There are three common substitutions among m19, m36 and m86: Pro, Arg and His replaced Ser at positions 305, 307 and 313, respectively (Table 2), indicating that these substitutions may be involved in binding of the C-CPE mutants to CL1. We prepared

Table 3
Sequences of m19 mutants.

	304	305	307	309	313	318
C-CPE	Ser	Ser	Ser	Asn	Ser	Lys
m19	Ala	Pro	Arg	His	His	Lys
Triple mutant	Ser	Pro	Arg	Asn	His	Lys
S305P	Ser	Pro	Ser	Asn	Ser	Lys
S307R	Ser	Ser	Arg	Asn	Ser	Lys
S313H	Ser	Ser	Ser	Asn	His	Lys
S305P/S307R	Ser	Pro	Arg	Asn	Ser	Lys
S305P/S313H	Ser	Pro	Ser	Asn	His	Lys
S307R/S313H	Ser	Ser	Arg	Asn	His	Lys

We prepared C-CPE mutants that contained single or double substituted amino acids.

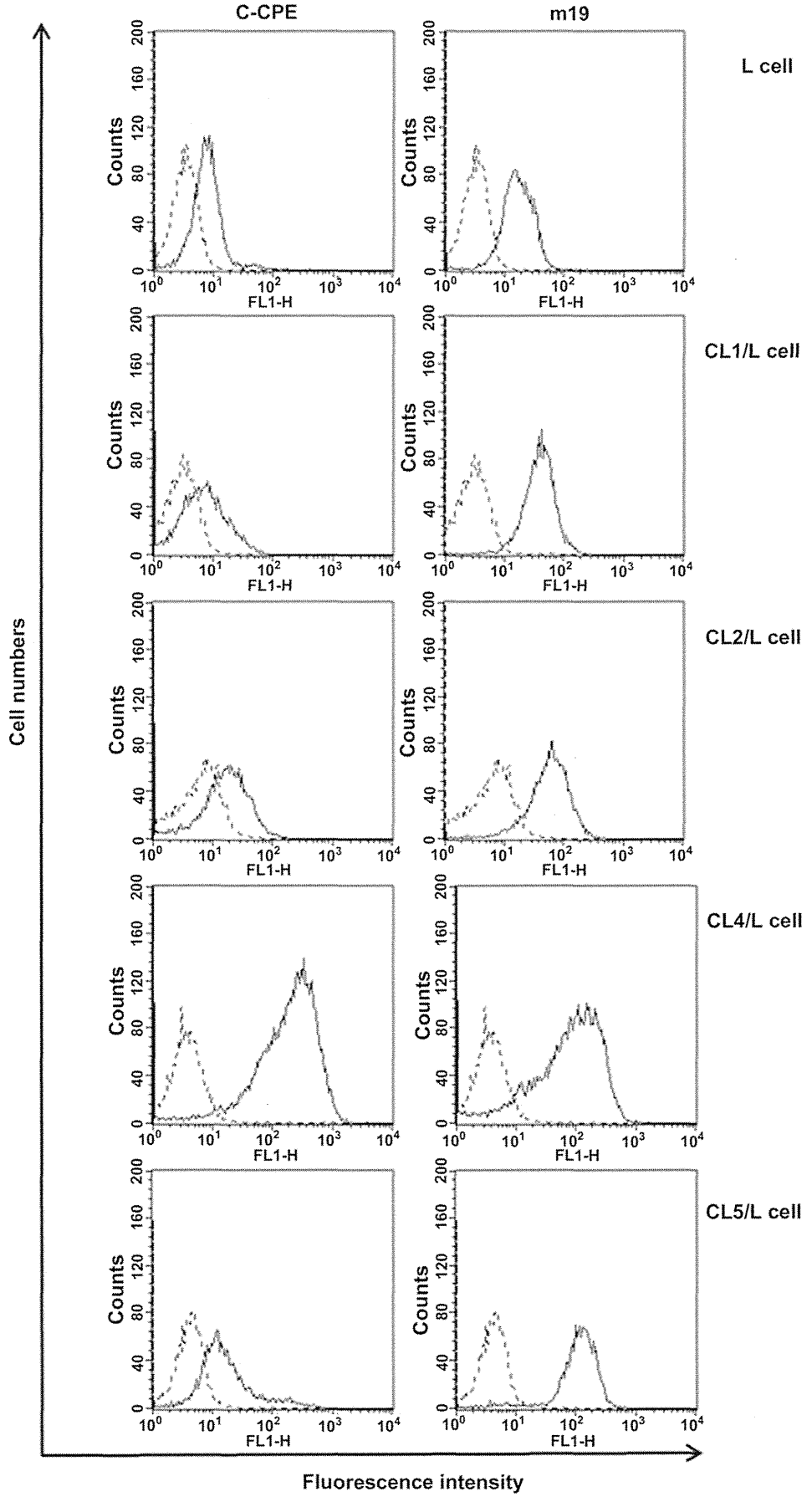

Fig. 4. FACS analysis of the interaction between m19 and CLs-cells. CLs-L cells were treated with C-CPE or m19. The bound C-CPE or m19 was detected by labeled secondary antibodies. Lined histograms indicate the level of reactivity of C-CPE or m19; dotted lined histograms indicate background binding level of anti-his tag and FITC-labeled antibodies without C-CPE or m19. The binding cells were detected by FACS analysis as described in the Materials and Methods.

a triple substituted C-CPE mutant with the same three common mutations: the triple mutant bound to CL1-BV but not to wild-BV (Fig. 3A). We prepared a series of single or double-substituted mutants (Table 3). All of the single and double mutants bound to CL1-BV (Fig. 3B). The double substituted mutant at 307 and 313 had the highest affinity to CL1-BV among the mutants (Fig. 3B). These findings indicate that Arg and His at positions 307 and 313, respectively, might be critical for the interaction of the C-CPE mutants with CL1. The isoelectric point (pI) values of Ser, Arg and His were 5.68, 10.76 and 7.59, respectively. We prepared a series of double substituted C-CPE mutants, changing Ser resides to His (pI, 7.59), Lys (pI, 9.8) or Arg (pI, 10.76), to investigate the effect of charge at positions 307 and 313 on CL1-binding. Increase and decrease in the charge at position 307 and 313, respectively, strengthened the interaction with CL1 (Fig. 3C). We also prepared double Ala- or Asp-substituted C-CPE mutants at position 307 and 313 (Ala, pI: 6.0; Asp, pI: 2.77); decrease in the charge attenuated binding to CL1 (Fig. 3D). These findings are consistent with the structural analysis of m19. Therefore, an electrostatic interaction may be involved in the binding of C-CPE mutants to CL1.

m19 interacts with CL1 via electrostatic forces, thus other CL members with a negatively charged C-CPE binding region may interact with m19. A series of chimeric analyses revealed that the region of CLs from the Asn at position 149 to the Met at position 160 may determine sensitivity of CPE (CPE sensitivity-related region; CPE-SR) [47]. The pI values of CPE-SRs are 9.70, 4.18, 4.18 and 4.18 in CL4, CL1 CL2 and CL5, respectively. A FACS analysis in CLs-expressing cells confirmed the CL member specificity for m19. C-CPE bound to CL4 but not CL1, CL2 and CL5. In contrast, m19 bound to CL1, CL2, CL4 or CL5-expressing cells (Fig. 4). Therefore, m19 may be a more broadly specific CL binder.

3.4. Effects of m19 on epithelial barriers

Caco-2 monolayer cell sheets are a common model for the evaluation of TJ barriers [48]. We compared the TJ-barrier–modulating activity of m19 and C-CPE in Caco-2 monolayer cell sheets. Treatment of the cells with C-CPE or m19 resulted in decreased TEER values (Fig. 5A); after removal of C-CPEs, the TEER values increased (Fig. 5B). The TJ-barrier-modulating activity of 20 μg/ml m19 was comparable to that of 50 μg/ml C-CPE, which indicates that m19 had stronger TJ-barrier-modulating activity than C-CPE.

There are two intercellular contacts in epithelial monolayer cell sheets: the bicellular junction between two adjacent cells and the tricellular junction on the corners at which three adjacent cells are joined [49,50]. The epithelial barrier is composed of bicellular junctions and tricellular junctions. Tricellulin is a key and functional component of tricellular junctions [51]. Tricellulin interacts with CLs in the plasma membrane [52]. We investigated the influence of m19 on epithelial barrier function in an epithelial barrier model using bicellularly tricellulin-expressing MDCK II cells developed by Krug et al. [35]. Treatment of MDCK II cells over-expressing tricellulin (TRa-8) or vector controls (V1) with 20 μg/ml C-CPE or m19 decreased the TEER values (Fig. 6A). A detailed characterization of TEER by two-path impedance spectroscopy revealed that the decrease was associated with a strong decrease of the paracellular resistance (R^{para}), while the transcellular resistance (R^{trans}) remained unchanged in both V1 cells and Tra-8 cells (Fig. 6B and C). This led to a decrease in the epithelial resistance (R^{epi}), which is TEER after subtraction of the subcellular resistance given by the filter supports (Fig. 6B and C). These findings indicate that m19 enhanced the paracellular permeability. Additional macromolecular fluxes supported the fact that C-CPE and m19 interact with CLs but not with tricellulin, as the permeability for FD-4 remained unchanged after C-CPE or m19 incubation (Fig. 6D).

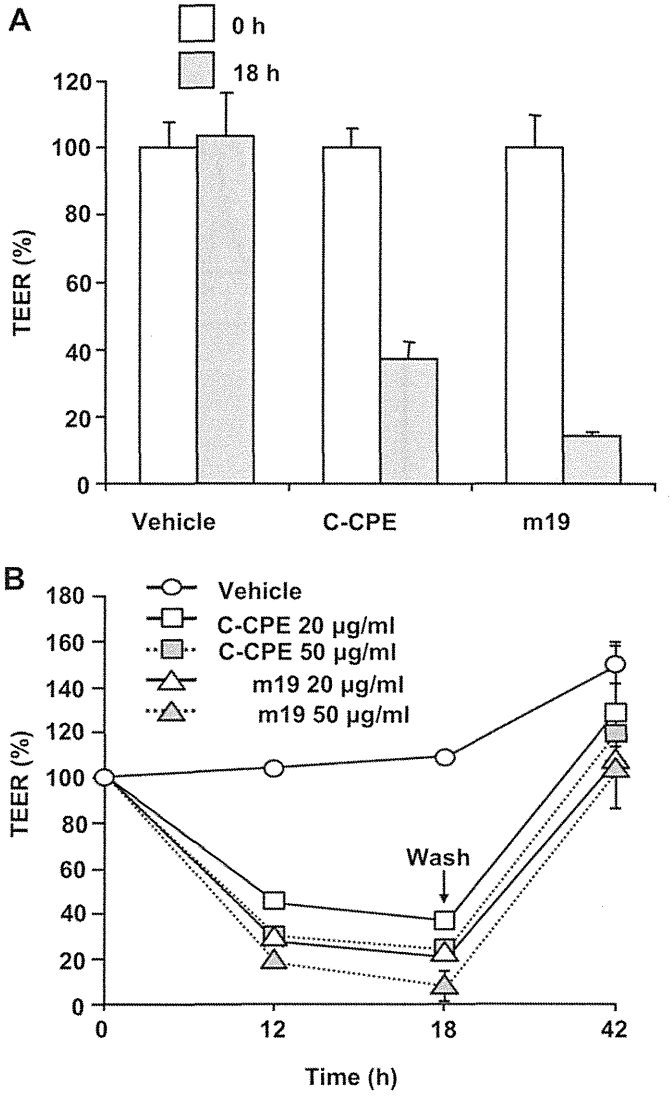

Fig. 5. Effect of m19 on TJ-integrity in Caco-2 monolayer cell sheets. A, B) Trans-epithelial electrical resistance (TEER) measurement. Caco-2 cells were seeded in BD BioCoat™ Fibrillar Collagen Cell Culture Inserts (BD Biosciences, Franklin Lakes, NJ) at a subconfluent density. The TEER of the Caco-2 monolayer cell sheets on the chamber was monitored with a Millicell-ERS epithelial volt-ohmmeter (Millipore, Billerica, MA). The Caco-2 monolayers were cultured for 5 days, and then treated with C-CPE or m19 on the basal side of the insert. The cells were exposed to the C-CPEs for 18 h (A), washed with medium to remove C-CPEs, and then cultured for an additional 24 h. Changes in TEER values were monitored during the C-CPE treatment (B). Relative TEER values were calculated as the ratio of TEER values at 0 h. The TEER values were normalized by the area of the Caco-2 monolayer, and the TEER value of a blank Transwell™ chamber (background) was subtracted. Data are presented as means ± SD ($n = 3$).

Thus, the observed effects were not mediated by tricellulin. C-CPE and m19 had similar TJ-barrier modulating activities. The discrepancy between Caco-2 cells and the MDCK cells will be addressed in the Discussion section.

We investigated effects of m19 on the localization of TJ-components by using anti-occludin, anti-tricellulin, and anti-CL1, 2, 3, 4, and 7 antibodies in an immunofluorescent analysis: there were no observable changes in the localization of each of the analyzed TJ proteins in the C-CPE or m19-treated cells (Fig. 7A–D, Suppl. Fig. 2A–H), indicating that disruption of the paracellular barrier may be due to inhibition of the adjacent intercellular interaction of CL strands caused by their interaction with the extracellular domains of CL.

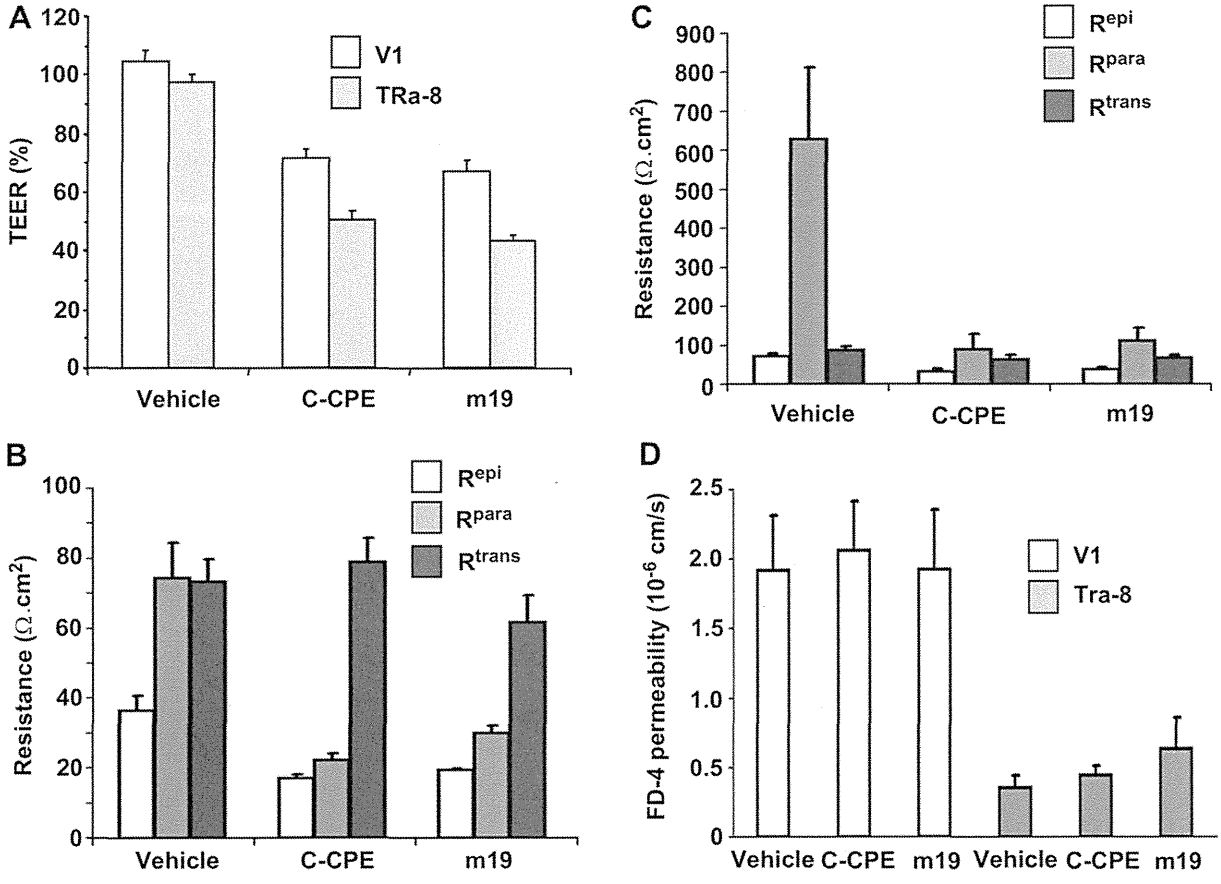

Fig. 6. Effects of m19 on the epithelial barrier in tricellulin-overexpressing MDCK II cells. A) TEER assay. Mock-expressing MDCK II cells (V1) or tricellulin-expressing MDCK II cells (TRa-8) were treated with C-CPE or m19 at 20 μg/ml for 3 h. The TEER was measured at 2 and 3 h. The TEER changes between 2 and 3 h were calculated as the ratio of TEER value at 2 h. The TEER was measured as described in Materials and Methods. Data are presented as means ± SE (n = 12–17). B, C) Effects of m19 on the paracellular resistance. V1 cells (B) or TRa-8 cells (C) were subjected to two-path impedance spectroscopy analysis as described in Materials and Methods. Data are presented as means ± SE (n = 5 or 6). D) Permeability for FD-4. V1 cells or TRa-8 cells were treated with C-CPE or m19 at 20 μg/ml for 3 h and flux for FD-4 was determined as described in Materials and Methods. Data are presented as means ± SE (n = 6 or 7).

3.5. Mucosal absorption-enhancing effects of m19

Finally, we investigated the effect of m19 on jejunal absorption by using an *in situ* loop assay and dextran with a molecular mass of 4000 Da (FD-4) as a model drug. C-CPE treatment increased plasma FD-4 levels in a time-dependent manner, reaching a maximal concentration of 3.0 μg/ml; in contrast, m19 enhanced jejunal absorption of FD-4 more than C-CPE, reaching a maximal concentration of 5.3 μg/ml (Fig. 8A). The AUC value of the m19-treated group was 2.1-fold that of the C-CPE-treated group (Fig. 8B). These results suggest that m19 is a more potent mucosal absorption enhancer than C-CPE.

4. Discussion

CL is a promising target for pharmaceutical therapy. However, CL has low antigenicity, and most attempts to prepare a monoclonal antibody against the extracellular loop region of CL have been unsuccessful. The three-dimensional structure of CL has never been determined, so it is impossible to perform a theoretical design of a CL binder based on structural information. We developed a screening system for CL binders by using a BV system and a C-CPE phage display library [30]. We successfully identified C-CPE mutants that bind to CL1, CL2, CL4 and CL5 by using this screening system. We determined the functional domain, and evaluated effects of the CL binder on modulation of the TJ-barrier to enhance mucosal absorption.

Previous reports indicate that CPE shows almost no interaction with CL1 [21,47,53]. We identified three CL1-binding C-CPE mutants, m19, m36 and m86, in which there were three common substitutions of Ser residues for Pro, Arg and His at positions 305, 307 and 313, respectively. In particular, double substitutions of Ser with Arg and His at positions 307 and 313, respectively, are important for interaction with CL1. Kimura et al. found that the CPE-binding region of CL3/4 (CPE-sensitive region; CPE-SR) may be positively charged and the CL3/4-binding region of CPE may be negatively charged; they proposed an electrostatic interaction model [47]. The pI value of CPE-SR in CL1, CL3 and CL4 is 4.18, 6.53 and 9.70, respectively [47]. Therefore, one possible explanation for binding of the C-CPE mutants to CL1 may be the increase of positively charged residues in the CL-binding region. C-CPE has 9 β-sheets and 1 α-helix, and the loop domain between β8- and β9-sheets may be the CL-binding domain [46]. Ser residues at positions 307 and 313 are located in the loop domain and the β9 sheet, respectively; changing Ser residues to Arg and His, respectively, may form a more positively charged CL-binding domain than C-CPE, leading to increased binding to CL1. Indeed, substitution of these Ser residues with Ala (pI, 6.0) or Asp (pI, 2.77) did not allow binding to CL1. These findings suggest that electrostatic interactions between C-CPE mutants and CL1 may be partially involved in their binding. In fact, the pI value of CPE-SR in CL5 was similar (4.18) to that of CL1, and also bound to

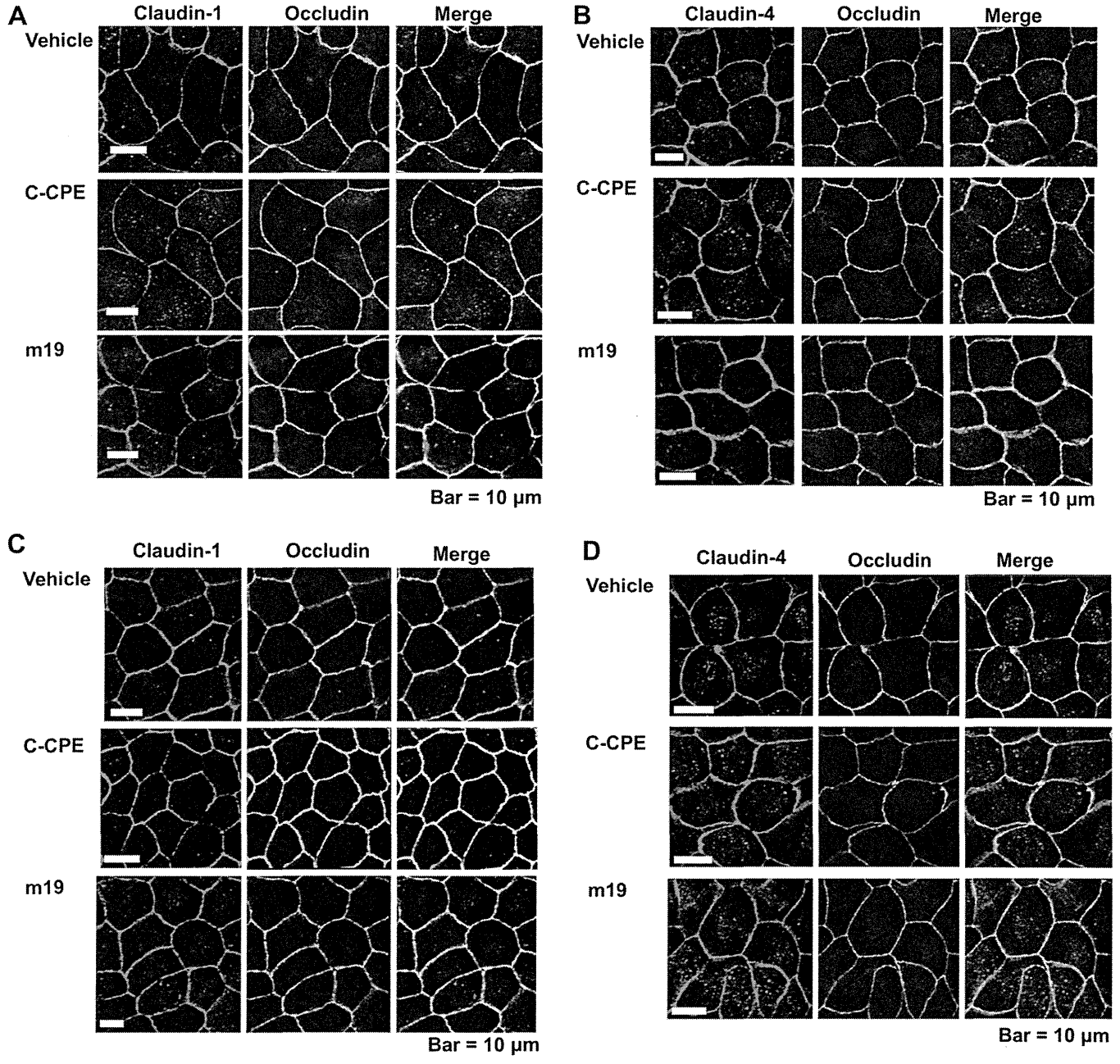

Fig. 7. Effects of m19 on localization of TJ-components. V1 cells (A, B) or TRa-8 cells (C, D) were treated with C-CPE or m19 at 20 μg/ml for 4 h. The cells were fixed with methanol and analyzed by immunofluorescence as described in Materials and Methods. CL1 (A and C), CL4 (B and D). CLs are stained red, and occludin green. Occludin was used as a TJ-marker.

m19. CL4 may interact with C-CPE at Tyr residues at positions 306, 310 and 312 and Leu at position 315. These residues form a negatively charged cleft [47]. Substitution of Ser with Arg at position 307 and Ser with His at position 313 may be important for the interaction of m19 with CL1. The binding motif for CL1 and CL4 may be different in m19. The cleft for CL4 might have a wide surface. In contrast, the motif for CL1 might be much smaller than that of CL4. An ELISA assay showed that m19 interacted much more weakly with CL1 than with CL4 (data not shown). These amino acid changes could also affect the secondary structure of the binding, which could then alter the binding affinity. Further kinetic and structural analyses of the interaction between m19 and CLs are needed.

Compared to C-CPE, m19 showed higher TJ-modulating activity in Caco-2 monolayer cell sheets and jejunal absorption-enhancing activity in rat; however, m19 showed similar TJ-modulating activity in MDCK II cells. Expression of CL4, 11 or 15 increases TJ-integrity in MDCK II cells. In contrast, expression of CL4 increases TJ-integrity in LLC-PK1 cells, but expression of CL11 or 15 decreases it [54]. CL5 is ubiquitously expressed in endothelial cells and is critical for the blood-brain-barrier [12,55]. Therefore, the difference in the activity of m19 may be due to differences in the properties of the TJ-seals in each of the assay systems: Caco-2 cells are human colon cells, MDCK II cells are canine kidney cells and rat jejunum is used in mucosal absorption of dextran.

Tricellulin has been shown to interact with CLs in the plasma membrane [52], but eventual changes in interaction due to binding of C-CPEs to CLs had no effect on macromolecular permeability regulated by tricellulin. Tricellulin also was excluded as interaction

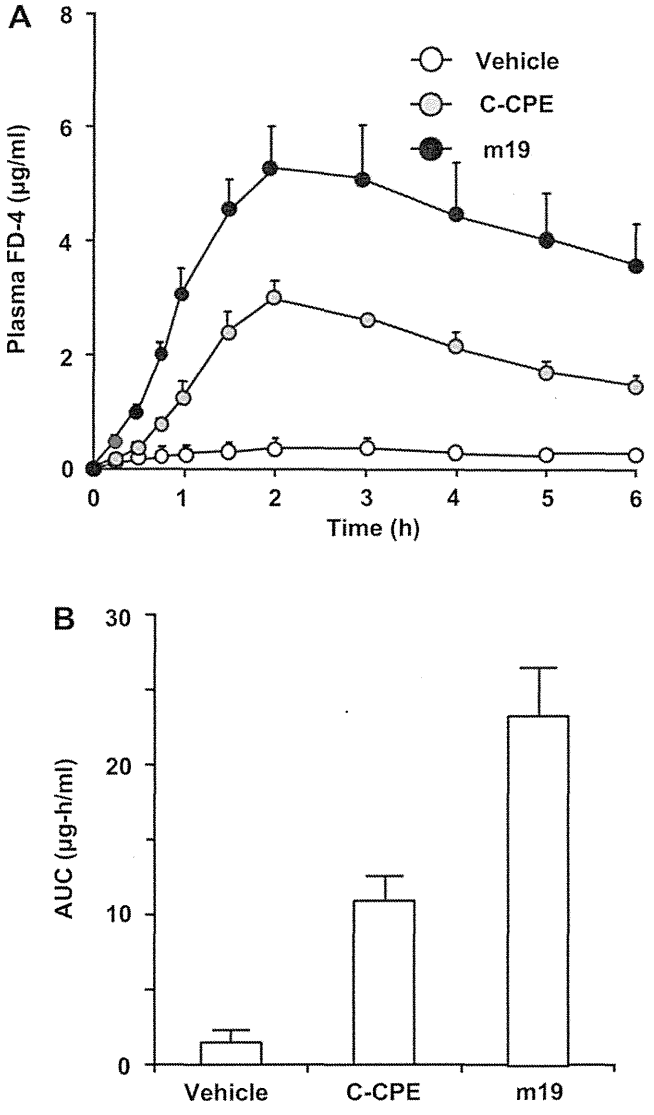

Fig. 8. Mucosal absorption of FD-4 by m19. Jejunum were treated with 2.0 mg/ml FD-4 and C-CPEs. Time-course changes in plasma FD-4 levels (A) and AUC from 0 to 6 h (B) were analyzed as described in Materials and Methods. Data are presented as means ± SE ($n = 4–9$).

partner for C-CPE and m19. Therefore effects that were not reflected by the cell culture model are responsible for the increase of macromolecular permeability in the jejunum which is not determined by CLs.

Preparation of CL is a requisite for screening CL binders. However, CL4 is the only CL with an established preparation method [56]. We attempted to screen the C-CPE mutant library by using CL1-expressing cells, but we did not successfully identify CL1 binders. Functional membrane proteins such as cell-surface proteins are heterologously expressed in their native forms on BVs [33,34,57]. Interactions between membrane proteins can be detected by using receptor-displaying and ligand-displaying BV [34]. CL-BV can work as a screen for CL binders by using CL4-BV and a CL4 binder, C-CPE [30]. The present study successfully identified CL1 binders from the library by using CL1-BV. We anticipate that CL-BV will be useful for the preparation of peptides and antibodies that act as CL binders.

Several groups have successfully prepared CL binders. Offner et al. prepared polyclonal antibodies against the extracellular domains of CL3 and CL4 [58], Ling et al. screened CL4 binding peptides by using a 12-mer peptide phage display library and CL4-expressing cells [59], and and Romani et al. screened scFv against CL3 by using a human antibody phage display library [60]. Suzuki et al. developed monoclonal antibodies to CL4 and CL3/4 by using mice with autoimmune disease [61,62]. Fofana et al. established a monoclonal antibody to CL1, which prevented infection by Hepatitis C virus in hepatocytes [63]. However, the TJ-modulating activities of these CL binders have never been reported; thus, C-CPE and its mutants, including m19, were the only known CL modulators [20]. The findings of the present study indicate that a BV screening system with a C-CPE library may be a powerful method to develop CL modulators.

5. Conclusions

We report here the preparation of broadly specific CL binders to CL1, CL2, CL4 and CL5. The electrostatic charge in the loop region between the β8 and β9 sheets may be critical for the interaction between the C-CPE mutants and CLs. The optimal modulation of the electrostatic charge of the CL binding region of C-CPE is an important part of the strategy for development of CL binders, contributing to CL-targeted drug development.

Acknowledgements

We thank Drs. S. Tsunoda (National Institute of Biomedical Innovation, Japan) and Y. Tsutsumi (Osaka University, Japan) for their kind instructions on the use of phage display technology. We also thank Drs. Y. Horiguchi (Osaka University, Japan), S. Tsukita (Kyoto University, Japan) and members of our laboratory for providing us C-CPE cDNA, CL-expressing cells and their useful comments and discussion, respectively. This work was supported by a Grant-in-Aid for Scientific Research from the Ministry of Education, Culture, Sports, Science and Technology, Japan (21689006), and by a Health and Labor Sciences Research Grant from the Ministry of Health, Labor and Welfare of Japan. A.T. and H.S. are supported by Research Fellowships from the Japan Society for the Promotion of Science for Young Scientists.

We thank beamline staff of BL44XU at SPring-8 for X-ray data collection. We also thank Academia Sinica and National Synchrotron Radiation Research Center (Taiwan) for use MX225-HE detector at BL44XU.

Appendix. Supplementary material

Supplementary material associated with this article can be found, in the online version, at doi:10.1016/j.biomaterials.2012.01.017.

References

[1] Farquhar MG, Palade GE. Junctional complexes in various epithelia. J Cell Biol 1963;17:375–412.
[2] Cassidy MM, Tidball CS. Cellular mechanism of intestinal permeability alterations produced by chelation depletion. J Cell Biol 1967;32:685–98.
[3] Wodarz A, Nathke I. Cell polarity in development and cancer. Nat Cell Biol 2007;9:1016–24.
[4] Yuki Y, Kiyono H. New generation of mucosal adjuvants for the induction of protective immunity. Rev Med Virol 2003;13:293–310.
[5] Jepson MA, Clark MA, Hirst BH. M cell targeting by lectins: a strategy for mucosal vaccination and drug delivery. Adv Drug Deliv Rev 2004;56:511–25.
[6] Ryan EJ, Daly LM, Mills KH. Immunomodulators and delivery systems for vaccination by mucosal routes. Trends Biotechnol 2001;19:293–304.
[7] Schneeberger EE, Lynch RD. The tight junction: a multifunctional complex. Am J Physiol 2004;286. C1213–C1228.
[8] Furuse M, Tsukita S. Claudins in occluding junctions of humans and flies. Trends Cell Biol 2006;16:181–8.
[9] Mineta K, Yamamoto Y, Yamazaki Y, Tanaka H, Tada Y, Saito K, et al. Predicted expansion of the claudin multigene family. FEBS Lett 2011;585:606–12.

[10] Furuse M, Sasaki H, Tsukita S. Manner of interaction of heterogeneous claudin species within and between tight junction strands. J Cell Biol 1999;147:891–903.
[11] Furuse M, Hata M, Furuse K, Yoshida Y, Haratake A, Sugitani Y, et al. Claudin-based tight junctions are crucial for the mammalian epidermal barrier: a lesson from claudin-1-deficient mice. J Cell Biol 2002;156:1099–111.
[12] Nitta T, Hata M, Gotoh S, Seo Y, Sasaki H, Hashimoto N, et al. Size-selective loosening of the blood-brain barrier in claudin-5-deficient mice. J Cell Biol 2003;161:653–60.
[13] Morin PJ. Claudin proteins in human cancer: promising new targets for diagnosis and therapy. Cancer Res 2005;65:9603–6.
[14] Rajapaksa TE, Stover-Hamer M, Fernandez X, Eckelhoefer HA, Lo DD. Claudin 4-targeted protein incorporated into PLGA nanoparticles can mediate M cell targeted delivery. J Control Release 2010;142:196–205.
[15] Tamagawa H, Takahashi I, Furuse M, Yoshitake-Kitano Y, Tsukita S, Ito T, et al. Characteristics of claudin expression in follicle-associated epithelium of Peyer's patches: preferential localization of claudin-4 at the apex of the dome region. Lab Invest 2003;83:1045–53.
[16] Evans MJ, von Hahn T, Tscherne DM, Syder AJ, Panis M, Wolk B, et al. Claudin-1 is a hepatitis C virus co-receptor required for a late step in entry. Nature 2007;446:801–5.
[17] McClane BA. *Clostridium perfringens* enterotoxin acts by producing small molecule permeability alterations in plasma membranes. Toxicology 1994;87:43–67.
[18] Katahira J, Inoue N, Horiguchi Y, Matsuda M, Sugimoto N. Molecular cloning and functional characterization of the receptor for *Clostridium perfringens* enterotoxin. J Cell Biol 1997;136:1239–47.
[19] Hanna PC, Wieckowski EU, Mietzner TA, McClane BA. Mapping of functional regions of *Clostridium perfringens* type A enterotoxin. Infect Immun 1992;60:2110–4.
[20] Sonoda N, Furuse M, Sasaki H, Yonemura S, Katahira J, Horiguchi Y, et al. *Clostridium perfringens* enterotoxin fragment removes specific claudins from tight junction strands: Evidence for direct involvement of claudins in tight junction barrier. J Cell Biol 1999;147:195–204.
[21] Fujita K, Katahira J, Horiguchi Y, Sonoda N, Furuse M, Tsukita S. *Clostridium perfringens* enterotoxin binds to the second extracellular loop of claudin-3, a tight junction integral membrane protein. FEBS Lett 2000;476:258–61.
[22] Uchida H, Kondoh M, Hanada T, Takahashi A, Hamakubo T, Yagi K. A claudin-4 modulator enhances the mucosal absorption of a biologically active peptide. Biochem Pharmacol 2010;79:1437–44.
[23] Kondoh M, Masuyama A, Takahashi A, Asano N, Mizuguchi H, Koizumi N, et al. A novel strategy for the enhancement of drug absorption using a claudin modulator. Mol Pharmacol 2005;67:749–56.
[24] Saeki R, Kondoh M, Kakutani H, Matsuhisa K, Takahashi A, Suzuki H, et al. A claudin-targeting molecule as an inhibitor of tumor metastasis. J Pharmacol Exp Ther 2010;334:576–82.
[25] Saeki R, Kondoh M, Kakutani H, Tsunoda S, Mochizuki Y, Hamakubo T, et al. A novel tumor-targeted therapy using a claudin-4-targeting molecule. Mol Pharmacol 2009;76:918–26.
[26] Ebihara C, Kondoh M, Hasuike N, Harada M, Mizuguchi H, Horiguchi Y, et al. Preparation of a claudin-targeting molecule using a C-terminal fragment of *Clostridium perfringens* enterotoxin. J Pharmacol Exp Ther 2006;316:255–60.
[27] Kakutani H, Kondoh M, Fukasaka M, Suzuki H, Hamakubo T, Yagi K. Mucosal vaccination using claudin-4-targeting. Biomaterials 2010;31:5463–71.
[28] Kominsky SL, Tyler B, Sosnowski J, Brady K, Doucet M, Nell D, et al. *Clostridium perfringens* enterotoxin as a novel-targeted therapeutic for brain metastasis. Cancer Res 2007;67:7977–82.
[29] Michl P, Buchholz M, Rolke M, Kunsch S, Lohr M, McClane B, et al. Claudin-4: a new target for pancreatic cancer treatment using *Clostridium perfringens* enterotoxin. Gastroenterology 2001;121:678–84.
[30] Kakutani H, Takahashi A, Kondoh M, Saito Y, Yamaura T, Sakihama T, et al. A novel screening system for claudin binder using baculoviral display. PLoS One 2011;6:e16611.
[31] Takahashi A, Komiya E, Kakutani H, Yoshida T, Fujii M, Horiguchi Y, et al. Domain mapping of a claudin-4 modulator, the C-terminal region of C-terminal fragment of *Clostridium perfringens* enterotoxin, by site-directed mutagenesis. Biochem Pharmacol 2008;75:1639–48.
[32] Takahashi A, Kondoh M, Masuyama A, Fujii M, Mizuguchi H, Horiguchi Y, et al. Role of C-terminal regions of the C-terminal fragment of *Clostridium perfringens* enterotoxin in its interaction with claudin-4. J Control Release 2005;108:56–62.
[33] Sakihama T, Masuda K, Sato T, Doi T, Kodama T, Hamakubo T. Functional reconstitution of G-protein-coupled receptor-mediated adenylyl cyclase activation by a baculoviral co-display system. J Biotechnol 2008;135:28–33.
[34] Sakihama T, Sato T, Iwanari H, Kitamura T, Sakaguchi S, Kodama T, et al. A simple detection method for low-affinity membrane protein interactions by baculoviral display. PLoS ONE 2008;3:e4024.
[35] Krug SM, Amasheh S, Richter JF, Milatz S, Günzel D, Westphal JK, et al. Tricellulin forms a barrier to macromolecules in tricellular tight junctions without affecting ion permeability. Mol Biol Cell 2009;20:3713–24.
[36] Battye TG, Kontogiannis L, Johnson O, Powell HR, Leslie AG. iMOSFLM: a new graphical interface for diffraction-image processing with MOSFLM. Acta Crystallogr D Biol Crystallogr 2011;67:271–81.
[37] Evans P. Scaling and assessment of data quality. Acta Crystallogr D Biol Crystallogr 2006;62:72–82.
[38] Winn MD, Ballard CC, Cowtan KD, Dodson EJ, Emsley P, Evans PR, et al. Overview of the CCP4 suite and current developments. Acta Crystallogr D Biol Crystallogr 2011;67:235–42.
[39] Long F, Vagin AA, Young P, Murshudov GN. BALBES: a molecular-replacement pipeline. Acta Crystallogr D Biol Crystallogr 2008;64:125–32.
[40] Emsley P, Cowtan K. Coot: model-building tools for molecular graphics. Acta Crystallogr D Biol Crystallogr 2004;60:2126–32.
[41] Murshudov GN, Vagin AA, Dodson EJ. Refinement of macromolecular structures by the maximum-likelihood method. Acta Crystallogr D Biol Crystallogr 1997;53:240–55.
[42] Krug SM, Fromm M, Gunzel D. Two-path impedance spectroscopy for measuring paracellular and transcellular epithelial resistance. Biophys J 2009;97:2202–11.
[43] Amasheh M, Grotjohann I, Amasheh S, Fromm A, Soderholm JD, Zeitz M, et al. Regulation of mucosal structure and barrier function in rat colon exposed to tumor necrosis factor alpha and interferon gamma in vitro: a novel model for studying the pathomechanisms of inflammatory bowel disease cytokines. Scand J Gastroenterol 2009;44:1226–35.
[44] Kirschner N, Houdek P, Fromm M, Moll I, Brandner JM. Tight junctions form a barrier in human epidermis. Eur J Cell Biol 2010;89:839–42.
[45] Kominsky SL. Claudins: emerging targets for cancer therapy. Expert Rev Mol Med 2006;8:1–11.
[46] Van Itallie CM, Betts L, Smedley 3rd JG, McClane BA, Anderson JM. Structure of the claudin-binding domain of *Clostridium perfringens* enterotoxin. J Biol Chem 2008;283:268–74.
[47] Kimura J, Abe H, Kamitani S, Toshima H, Fukui A, Miyake M, et al. *Clostridium perfringens* enterotoxin interacts with claudins via electrostatic attraction. J Biol Chem 2010;285:401–8.
[48] Meunier V, Bourrie M, Berger Y, Fabre G. The human intestinal epithelial cell line Caco-2; pharmacological and pharmacokinetic applications. Cell Biol Toxicol 1995;11:187–94.
[49] Staehelin LA. Further observations on the fine structure of freeze-cleaved tight junctions. J Cell Sci 1973;13:763–86.
[50] Staehelin LA, Mukherjee TM, Williams AW. Freeze-etch appearance of the tight junctions in the epithelium of small and large intestine of mice. Protoplasma 1969;67:165–84.
[51] Ikenouchi J, Furuse M, Furuse K, Sasaki H, Tsukita S, Tsukita S. Tricellulin constitutes a novel barrier at tricellular contacts of epithelial cells. J Cell Biol 2005;171:939–45.
[52] Ikenouchi J, Sasaki H, Tsukita S, Furuse M, Tsukita S. Loss of occludin affects tricellular localization of tricellulin. Mol Biol Cell 2008;19:4687–93.
[53] Winkler L, Gehring C, Wenzel A, Müller SL, Piehl C, Krause G, et al. Molecular determinants of the interaction between *Clostridium perfringens* enterotoxin fragments and claudin-3. J Biol Chem 2009;284:18863–72.
[54] Van Itallie CM, Fanning AS, Anderson JM. Reversal of charge selectivity in cation or anion-selective epithelial lines by expression of different claudins. Am J Physiol 2003;285:F1078–84.
[55] Morita K, Furuse M, Fujimoto K, Tsukita S. Claudin multigene family encoding four-transmembrane domain protein components of tight junction strands. Proc Natl Acad Sci U S A 1999;96:511–6.
[56] Mitic LL, Unger VM, Anderson JM. Expression, solubilization, and biochemical characterization of the tight junction transmembrane protein claudin-4. Protein Sci 2003;12:218–27.
[57] Loisel TP, Ansanay H, St-Onge S, Gay B, Boulanger P, Strosberg AD, et al. Recovery of homogeneous and functional beta 2-adrenergic receptors from extracellular baculovirus particles. Nat Biotechnol 1997;15:1300–4.
[58] Offner S, Hekele A, Teichmann U, Weinberger S, Gross S, Kufer P, et al. Epithelial tight junction proteins as potential antibody targets for pan-carcinoma therapy. Cancer Immunol Immunother 2005;54:431–45.
[59] Ling J, Liao H, Clark R, Wong MS, Lo DD. Structural constraints for the binding of short peptides to claudin-4 revealed by surface plasmon resonance. J Biol Chem 2008;283:30585–95.
[60] Romani C, Comper F, Bandiera E, Ravaggi A, Bignotti E, Tassi RA, et al. Development and characterization of a human single-chain antibody fragment against claudin-3: a novel therapeutic target in ovarian and uterine carcinomas. Am J Obstet Gynecol 2009;201(70):e1–9.
[61] Kato-Nakano M, Suzuki M, Kawamoto S, Furuya A, Ohta S, Nakamura K, et al. Characterization and evaluation of the antitumour activity of a dual-targeting monoclonal antibody against claudin-3 and claudin-4. Anticancer Res 2010;30:4555–62.
[62] Suzuki M, Kato-Nakano M, Kawamoto S, Furuya A, Abe Y, Misaka H, et al. Therapeutic antitumor efficacy of monoclonal antibody against Claudin-4 for pancreatic and ovarian cancers. Cancer Sci 2009;100:1623–30.
[63] Fofana I, Krieger SE, Grunert F, Glauben S, Xiao F, Fafi-Kremer S, et al. Monoclonal anti-claudin 1 antibodies prevent hepatitis C virus infection of primary human hepatocytes. Gastroenterology 2010;139:953–64.

Virus Research 165 (2012) 214–218

Contents lists available at SciVerse ScienceDirect

Virus Research

journal homepage: www.elsevier.com/locate/virusres

Short communication

Suppression of hepatitis C virus replicon by adenovirus vector-mediated expression of tough decoy RNA against miR-122a

Fuminori Sakurai[a], Norihisa Furukawa[b], Maiko Higuchi[b], Sayuri Okamoto[a], Kaori Ono[a], Takeshi Yoshida[c], Masuo Kondoh[c], Kiyohito Yagi[c], Naoya Sakamoto[d], Kazufumi Katayama[a], Hiroyuki Mizuguchi[a,b,e,*]

[a] Laboratory of Biochemistry and Molecular Biology, Graduate School of Pharmaceutical Sciences, Osaka University, Osaka, Japan
[b] Laboratory of Stem cell Regulation, National Institute of Biomedical Innovation, Osaka, Japan
[c] Laboratory of Bio-functional Molecular Chemistry, Graduate School of Pharmaceutical Sciences, Osaka University, Osaka, Japan
[d] Department of Gastroenterology and Hepatology, Tokyo Medical and Dental University, Tokyo, Japan
[e] The Center for Advanced Medical Engineering and Informatics, Osaka University, Osaka, Japan

ARTICLE INFO

Article history:
Received 5 December 2011
Received in revised form 27 January 2012
Accepted 3 February 2012
Available online 10 February 2012

Keywords:
Adenovirus vector
Tough decoy RNA
miR-122a
Hepatitis C virus
microRNA

ABSTRACT

Recent studies have demonstrated that the liver-specific microRNA (miRNA) miR-122a plays an important role in the replication of hepatitis C virus (HCV). Antisense nucleotides against miR-122a, including locked nucleic acid (LNA), have shown promising results for suppression of HCV replication; however, a liver-specific delivery system of antisense nucleotides has not been fully developed. In this study, an adenovirus (Ad) vector that expresses tough decoy (TuD)-RNA against miR-122a (TuD-122a) was developed to suppress the HCV replication in the liver hepatocytes. Ad vectors have been well established to exhibit a marked hepatotropism following systemic administration. An in vitro reporter gene expression assay demonstrated that Ad vector-mediated expression of TuD-122a efficiently blocked the miR-122a in Huh-7 cells. Furthermore, transduction with the Ad vector expressing TuD-122a in HCV replicon-expressing cells resulted in significant reduction in the HCV replicon levels. These results indicate that Ad vector-mediated expression of TuD-122a would be a promising tool for treatment of HCV infection.

Hepatitis C virus (HCV) is a hepatotropic human virus belonging to a member of the family *Flaviviridae* and possessing a 9.6-kb positive-sense RNA genome. HCV infection causes chronic hepatic inflammation and fibrosis, leading to hepatocellular carcinoma (Hoofnagle, 2002). Currently, 170 million people worldwide are infected with HCV, and suffering from or at risk for the diseases described above. In order to suppress the replication of HCV, PEGylated interferon alpha and ribavirin, which is a nucleotide analogue, have been used as standard-of-care therapy; however, the therapeutic efficiency has been limited, in spite of relatively severe side effects, including fever and malaise (Chisari, 2005; Feld and Hoofnagle, 2005). Another therapeutic strategy should be developed to efficiently suppress the HCV infection and HCV-caused diseases.

Among several host factors involved in HCV infection, the abundant liver-specific microRNA (miRNA), miR-122a has been demonstrated to be crucial for efficient replication and/or translation of the HCV genome (Henke et al., 2008; Jopling et al., 2005; Randall et al., 2007). The HCV genome has two closely spaced miR-122a-binding sites in the 5′-untranslated region (UTR), which contains overlapping *cis*-acting signals involved in translation and RNA synthesis (Jopling et al., 2005). Although the mechanism of the miR-122a-mediated enhancement of HCV replication is controversial (Henke et al., 2008; Jopling et al., 2005; Machlin et al., 2011; Roberts et al., 2011; Wilson et al., 2011), antisense oligonucleotides complementary to miR-122a, including locked nucleic acid (LNA) oligonucleotides, have been shown to significantly inhibit miR-122a and reduce the HCV genome, and thereby to exhibit superior therapeutic effects (Henke et al., 2008; Jopling et al., 2005; Krutzfeldt et al., 2005; Lanford et al., 2010). Intravenous administration of LNA oligonucleotides against miR-122a into HCV-infected chimpanzees resulted in the long-lasting suppression of HCV viremia without viral resistance or severe side effects (Lanford et al., 2010). In addition, the 5′-UTR of the HCV genome is composed of highly conserved structural domains, suggesting that a mutant lacking the miR-122a-binding sites in the genome is unlikely to appear. These results indicate that miR-122a is a promising target for the treatment of HCV-related diseases; however, LNA oligonucleotides accumulate in the kidney immediately after intravenous administration and are excreted into the urine (Fluiter et al., 2003).

* Corresponding author at: Laboratory of Biochemistry and Molecular Biology, Graduate School of Pharmaceutical Sciences, Osaka University, 1-6 Yamadaoka, Suita, Osaka 565-0871, Japan. Tel.: +81 6 6879 8185; fax: +81 6 6879 8186.
E-mail address: mizuguch@phs.osaka-u.ac.jp (H. Mizuguchi).

0168-1702/$ – see front matter © 2012 Elsevier B.V. All rights reserved.
doi:10.1016/j.virusres.2012.02.003